Journal of Archaeological Science: Reports 46 (2022) 103705

Contents lists available at ScienceDirect

Journal of Archaeological Science: Reports

journal homepage: www.elsevier.com/locate/jasrep

High-resolution investigation of a conflagration event in the North-East Temple at Lachish via integration of forensic, stratigraphic and geoarchaeological evidence: A model for studying architectural destruction by fire

Igor Kreimerman [a,b,*], Yosef Garfinkel [a], Michael G. Hasel [c], Ruth Shahack-Gross [b,*]

[a] Institute of Archaeology, Hebrew University of Jerusalem, Mount Scopus, Jerusalem 9190501, Israel
[b] Department of Maritime Civilizations, Recanati Institute of Maritime Studies, School of Archaeology and Maritime Cultures, University of Haifa, Haifa 3498838, Israel
[c] Institute of Archaeology, Southern Adventist University, P.O.B. 370, Collegedale, TN 37315, USA

ARTICLE INFO

Keywords:
Destruction
Conflagration
FTIR
Fire investigation
Mud bricks
Lachish

ABSTRACT

Burnt structures are well known archaeologically throughout the Near East. This study proposes an integrated interpretational framework for reconstructing fires in mud-brick structures using macro- and micro-archaeological types of evidence employing well-established tools. While previous research often utilized either macroscopic field evidence or micro-geoarchaeological data, here we present the integration of stratigraphy, architecture and location of artefacts in the framework of archaeology of crisis, spatial reconstruction of fire temperatures using micro-geoarchaeology, insights from experimental archaeology, and concepts from fire investigation. We demonstrate the utility of this integrative framework in a high-resolution reconstruction of a destructive fire event that occurred in the Late Bronze Age North-East Temple at Tel Lachish, ca. 1210–1126 BCE. We identify the area of ignition and the fire propagation path, and propose the cause of the fire in relation to the archaeology and history of the site in the 12th century BCE.

1. Introduction

Destruction is a multi-faceted phenomenon that is especially prominent archaeologically where evidence of fire (e.g., ash, soot, burnt mud bricks) is uncovered (Driessen, 2013a). The interpretation of archaeological events of architectural destruction by fire has recently advanced owing to developments and application of micro-geoarchaeology, experimental archaeology, archaeomagnetism and fire investigation methods. In the Near East, where architectural destruction is prevalent in Bronze and Iron Age contexts in *tell* sites, these methods have often been applied separately to the study of the so-called 'destruction layers', archaeological conflagration remains often found across part or an entire occupation level of ancient cities. While a few previous studies in the Southern Levant, part of the Near East, have integrated stratigraphy, pottery assemblages and FTIR analysis, none to date have integrated forensic fire investigation with the former fields. This lack of integration hampers high-resolution reconstruction of ancient architectural conflagration events in Near Eastern archaeology.

This paper begins with a survey of the current state of research on the investigation of ancient architectural fires in ancient Near Eastern sites and highlights the existing gaps. Next, we present an integrative framework (summarized in Fig. 1) that can be used to deduce the development of fires in typical Near Eastern structures, built of stone, mud bricks and with mud-covered roofs. The framework utilizes the distribution of ash, soot, charred matter, burnt bricks and wall segments, and temperature maps reconstructed using Fourier Transform Infrared Spectroscopy (FTIR), together with insights from modern fire investigation (all of these techniques are well established). When overlaid on site plans and considering architecture, stratigraphy (e.g., floors vs fills), installations, pottery assemblages and presence/absence of artefact types, a high-resolution reconstruction of the events leading to the conflagration, during conflagration and after it can be deduced. Finally,

* Corresponding authors at: Institute of Archaeology, Hebrew University of Jerusalem, Mount Scopus, Jerusalem 9190501, Israel (I. Kreimerman). Department of Maritime Civilizations, Recanati Institute of Maritime Studies, School of Archaeology and Maritime Cultures, University of Haifa, Haifa 3498838, Israel (R. Shahack-Gross).
E-mail addresses: kreimerm.igor@mail.huji.ac.il (I. Kreimerman), rgross@univ.haifa.ac.il (R. Shahack-Gross).

https://doi.org/10.1016/j.jasrep.2022.103705
Received 1 June 2022; Received in revised form 25 September 2022; Accepted 21 October 2022

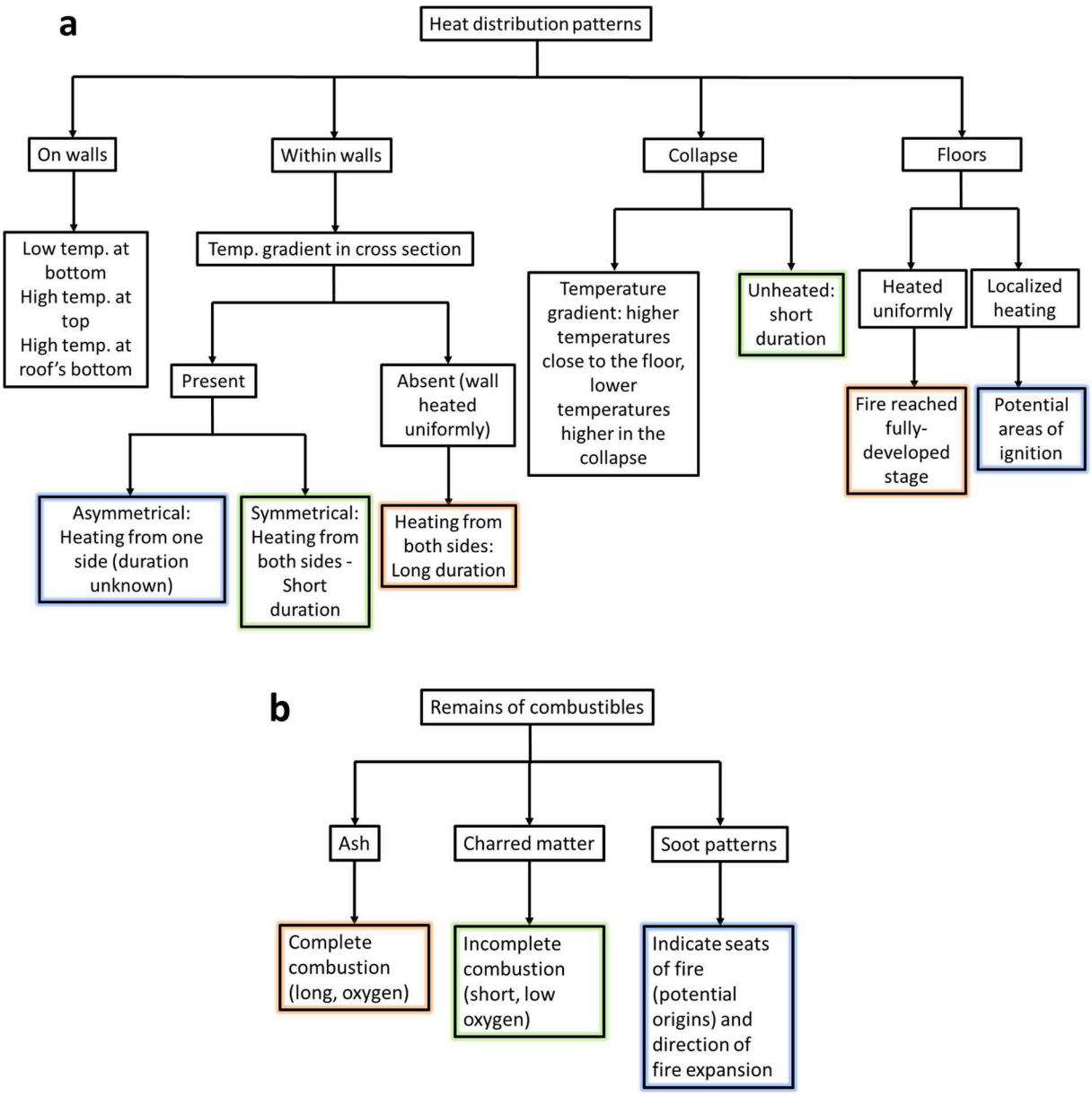

Fig. 1. Model summarizing the types of evidence that are instrumental for the investigation and reconstruction of the course of fire at archaeological sites, arranged in two categories: (a) Heat distribution patterns; (b) Remains of combustibles. Orange – evidence indicates long duration of fire; green – evidence indicates short duration of fire; blue – evidence might be used to infer direction of fire progress. (For interpretation of the references to colour in this figure legend, the reader is referred to the web version of this article.)

we demonstrate the use of this framework in a case study – the conflagration in the North-East Temple of Lachish.

1.1. State of research: Macroscopic evidence for architectural conflagration events

Burnt mud-brick or wattle-and-daub structures appear in the Near East as early as the Neolithic period (e.g., Stordeur et al., 2000; Verhoeven, 2000; Twiss et al., 2008). Although there is no standard definition of a destruction layer in the literature, the term usually refers to floors covered with charred wooden beams, other charred remains, ash, soot and mud-brick collapse and normally containing assemblages composed of crushed (restorable) pottery (Finkelstein, 2009).

Traditional study of conflagration events in the Bronze and Iron Age Near East is based on two approaches. The first is examination of evidence found at the field through visual observations such as the locations and thickness of ash and charred matter, burnt bricks and calcinated stones. By using this approach studies have noted that the extent and intensity of fire may differ between different rooms in a building, and different buildings at a site (e.g., Driessen and Macdonald, 1997; Seeher, 2001; Zuckerman, 2007; Finkelstein, 2009; Matthiae, 2009; Kreimerman, 2017a). Other studies have used field observations to reconstruct deposition sequences of burnt structures following standard stratigraphic principles and used these observations to identify the collapse of walls and roofs and time periods when buildings remained standing between fire and collapse (e.g., Mazar, 1980: 39; Adler, 2001: 54, 188; Puytison-Lagarce and Lagarce, 2006). Some scholars have attempted to use such evidence to reconstruct ancient fires, or to argue that fires were intentionally or accidentally set (e.g., Puytison-Lagarce and Lagarce, 2006; Arav, 2014; Millek, 2017). Yet, the lines of evidence used in these studies are sometimes insufficient to reach the suggested conclusions.

The second approach is to examine the circumstances prior to the conflagration and thus to infer the cause of fire in a building indirectly. Owing to a large extent to the pioneering works of Driessen (1995; 1999; 2013a, 2013b; Driessen and Macdonald, 1997), destruction is interpreted as part of a process. This approach assumes that by understanding the broader context of the destruction event it is possible to determine, even if not unequivocally, the cause of destruction. Several trajectories are considered especially useful for deciphering the events preceding destruction: (1) abandonment patterns; (2) crisis architecture; (3) evidence of battle; (4) indicators of earthquakes. These proxies are briefly discussed below.

Ethnographic and ethnoarchaeological studies on abandonment behaviour of settlements have highlighted the connection between the quantity of objects that when left were in usable condition, defined by Schiffer (1987: 89) as *de facto refuse*, and the abandonment process of the site. Generally, when sites are abandoned in an organised manner with no intention to return, few items are left on the floors – usually these are large objects that are difficult to carry or objects with low economic value. When abandonment is rapid, or with intention to return later, more *de facto refuse* is found – the faster the abandonment, the more items are left and the higher their economic value (LaMotta and Schiffer, 1999; Nelson and Schachner, 2002). Evidence of abandonment prior to the destruction, therefore, might hint that the fire did not come as a surprise and was anticipated by the residents, and hence was not accidental (Seeher, 2001; Hasel, 2016). The difficulty in this interpretation is that it is usually impossible to estimate the time between abandonment and destruction by fire, and so theoretically a structure could have been abandoned intentionally, but fire occurred much later from unrelated, possibly accidental, circumstances.

Driessen (1995) coined the term 'crisis architecture' to describe specific and sudden short-term architectural changes that come as a response to situations of social crisis. Driessen suggested three types of evidence for identifying crisis architecture: (a) decrease of energy input in production and maintenance, (b) change of original function and (c) change of original plan (Driessen, 1995: 67). These can be identified in the use of cheaper or scavenged building materials for construction, the partial abandonment of buildings, disrepair, inner partitioning of halls, restriction of access and the placement of domestic installations in corridors along the main axis of movement or in previously public spaces (Driessen, 1995: 67–76). Consequently, the presence of 'crisis architecture' might hint that destruction was a result not of a sudden and completely unexpected event (e.g., earthquake, sudden attack) but rather of a long process. Similarly, termination rituals could indicate change in the belief system (Bjorkman, 1999; Zuckerman, 2007), supporting the possibility of the inhabitants themselves being responsible for the fire and thus reducing the probability that fire was accidental.

Most traditional studies also use the presence of arrowheads or trapped skeletons showing evidence of trauma by sharp objects to infer warfare as the context of destruction (e.g., Driessen, 1999; Wileman, 2009; Kreimerman, 2016; 2017b). The major challenge in this respect is that arrowheads are found only when a battle took place and normally at the location of the battle. When the location of the battle was not exposed by excavation or when the city had surrendered without battle, such evidence might be lacking (Kreimerman, 2016; 2022). Furthermore, it was a common practice after conquest to clean cities of corpses for reasons of hygiene (Kreimerman, 2017b). Thus, arrowheads and skeletons with signs of trauma are absent from many of the layers that are securely attributed to military campaigns based on historical accounts.

Evidence of earthquakes is routinely sought and several studies have established criteria for their identification in the archaeological record (e.g., Stiros, 1996; Marco, 2008; Rodríguez-Pascua et al., 2011). The major difficulty in Bronze and Iron Age Near Eastern sites is that unequivocal evidence for seismic activity is observed in only a few cases (Marco, 2008; Lazar et al., 2020), while the most common evidence in destruction layers, such as fallen walls, trapped skeletons and broken pottery, could be the result of human-induced destruction.

The two above-mentioned approaches for the study of conflagration events could be seen as complementary. Although not stated explicitly in previous archaeological studies, circumstantial and indirect considerations are used in modern fire investigation as well to infer whether fire resulted from arson or accident. Fire investigators are instructed to examine the inventory of the burnt building for items found in unusual locations or missing from the structure's expected inventory, and to identify blocked or obstructed entrances. Such evidence has to be explained and might hint that fire was not accidental. The personal circumstances of the structure's owner, for instance if he was experiencing social or financial crisis, are also taken into consideration as possible clues (NFPA 921: 24.3).

While traditional study of destruction layers has advanced our understanding of destruction as a cultural phenomenon, and occasionally supplies us indirect evidence for the cause of fire, it has not contributed to reconstruction of the fire events themselves.

1.2. State of research: Micro-geoarchaeology and the study of architectural destruction by fire

Table 1 and the brief summary below highlight the fact that studies that utilize micro-archaeological parameters have not so far applied up-to-date concepts from modern fire investigation to reconstruct ancient fires.

Especially developed in the Near East owing to the long-term use of infrared spectroscopy in micro-geoarchaeological research is the identification of several heat-altered minerals: clays, calcite and aragonite. Shoval et al. (1989) studied mud bricks and were the first to propose a method for reconstructing heat intensity from the infrared spectra of clay minerals. This was further developed by Berna et al. (2007), who applied it to the study of sediments (activity deposits). This method is nowadays routinely used to reconstruct heat in archaeological sites of the Lower Palaeolithic to the Middle Ages across the world (e.g., Berna et al., 2012; Godleman et al., 2016; Passerini et al., 2016; Hlubik et al., 2017; Rodríguez-Cintas and Cabanes, 2017; Sanz et al., 2017; Villagran et al., 2017; Dunseth et al., 2019). Following these guidelines, Forget et al. (2015) conducted a study focusing specifically on the effects of heat on clay in mud bricks, looking into parameters such as heat intensity, duration and atmosphere and contributing refined infrared as well as macroscopic criteria to the understanding of the collapse material and brick wall stubs found in excavated destruction levels.

Turning to the carbonate minerals, Regev et al. (2010) introduced a method enabling a distinction to be made between geogenic (e.g., limestone) and pyrogenic (e.g., wood ash and lime plaster) calcites. Aragonite may also be present at archaeological sites as a by-product of calcination at temperatures higher than 650 °C, dubbed 'pyrogenic aragonite' (Toffolo and Boaretto, 2014). Finally, aragonite may be present at archaeological sites as a primary component in the form of mollusc shells (marine and/or terrestrial) that upon heating at 450–700 °C transforms into calcite (Yoshioka and Kitano, 1985; Shahack-Gross et al., 2005: 1423; Aldeias et al., 2016).

The spatial distribution of these minerals — heat-altered clay, pyrogenic calcite and pyrogenic aragonite — has been successfully used in several studies of archaeological destruction layers in the Southern Levant (Table 1). Berna et al. (2007) used these methods to understand the heat regime across a section at Tel Dor. Namdar et al. (2011) employed this approach to understand the formation processes of a 3 × 5 m excavation unit at Tell es-Safi/Gath. Regev et al. (2015) used a similar approach coupled with phytolith analysis to identify activity areas, deposition sequences and map temperatures across their study area. Forget and Shahack-Gross (2016) used insights from experimental heating of mud bricks (Forget et al., 2015) to estimate the length of a conflagration event at Tel Megiddo. Shahack-Gross et al. (2018) used these criteria to support and amplify an archaeomagnetic study of mud bricks in a destruction level at Tel Megiddo. This archaeomagnetic study

Table 1
Summary of methods used in studies of destruction by fire mentioned in the text, arranged chronologically.

Site and context	Field evidence	Micro-geoarchaeology	Fire investigation	Remarks
Tel Hadar (Shoval et al. 1989)	—	√	—	Estimation only of temperatures and duration of conflagration using FTIR spectroscopy
Opovo (Stevanović 1997)	√	—	√ (outdated criteria)	Identification of ignition points and concluding that the fire resulted of arson
Ras Ibn-Hani (Puytison-Lagarce and Lagarce 2006)	√	—	—	Temperature estimation based on melting points of materials and fire reconstruction based on visual observations
Tel Dor, Phase G9 (Berna et al. 2007)	√	√	—	2D study of a section, estimation of temperatures using FTIR spectroscopy
Palaikastro (Cunningham, 2007)	√	—	√	Flashover identified based on molten pottery (fire propagation path and fire origin not determined)
Çatalhöyük (Harrison 2008;Twiss et al. 2008)	√	—	√	Reconstruction of fire based on unusual preservation of scorch and soot marks on plastered walls
Tell es-Safi/Gath, Layer A3 (Namdar et al. 2011)	√	√	—	3D study of deposition processes in a 15 m^2 area, temperature estimation using FTIR spectroscopy
Tel Megiddo, Level Q4 (Regev et al. 2015)	√	√	—	Mapping of temperatures using FTIR spectroscopy, activity areas and deposition sequences but without reconstruction of the fire itself
Megiddo Q7 (Forget et al. 2015; Forget and Shahack-Gross 2016; Shahack-Gross et al. 2018)	√	√	—	Focused on the effect of fire on mud bricks using FTIR spectroscopy and mud-brick wall segments within a 200 m^2 area
Tel 'Eton (Faust et al. 2017; Sapir et al. 2018)	√	√	—	Focused on construction techniques and activity areas in a complete building, temperatures mapped across a structure using FTIR spectroscopy but fire propagation path was not reconstructed
Erimi (Amadio et al. 2020)	√	√	—	Reconstruction of a conflagration event in a 54 m^2 single room space using FTIR spectroscopy and micromorphology

addressed the question of whether burned mud-brick walls are the result of construction with sun-dried mud bricks and later burning as one unit, or construction with pre-fired bricks. The authors demonstrated that construction was carried out with sun-dried mud bricks and that certain burned wall segments were uniformly heated throughout, despite their high volume and the low heat conductance of clay. A study conducted at Tel 'Eton examined the temperatures to which walls and sediments were exposed in an entire structure, but did not aim at reconstructing the fire event (Faust et al., 2017; Sapir et al., 2018). Most recently, Amadio et al. (2020) applied geoarchaeological methods to study formation processes at Erimi (Cyprus) and offered a reconstruction of a conflagration event in a 54 m^2 single-room structure. Their interpretation of this event, however, might have benefited from consideration of fire behaviour in closed compartments (see 1.5.1 below).

It is noted that micromorphology, an important technique in micro-geoarchaeology, is rarely applied to the study of architectural conflagration. Previous studies have applied this technique to identify materials and the deposition sequence, and to better characterize the various layers observed. Namdar et al. (2011) showed micromorphologically that the black layer found directly on the floor of destroyed structures is composed of rolled charcoal fragments, probably indicating post-abandonment movement (rolling) of charcoal across abandoned floors. Regev et al. (2015) identified a micro-stratigraphic sequence showing that a burning vegetal roof collapsed on a structure's floor and thus scorched it and caused charring of organic components that were present within the floor makeup. While micromorphology can provide such glimpses into conflagration in large architectural units, it is quite a laborious method (relatively lengthy laboratory preparation followed by expert microscopic analysis) and therefore cannot be used to cover large portions of a destroyed structure. It best complements bulk analyses (such as FTIR spectroscopy) that can be conducted faster and in a higher sampling resolution. Using both methods is quite advantageous for gaining a full picture of the destruction event (e.g., Amadio et al., 2020).

As Table 1 shows, recent micro-geoarchaeological studies of conflagration events in the Bronze and Iron Age Southern Levant and Cyprus have focused on heat patterns using FTIR spectroscopy. Although this well-established approach was applied to many studies, reconstruction of the conflagration event itself in these contexts did not benefit from integration fire investigation concepts and knowledge.

1.3. State of research: Fire investigation and archaeology

Some archaeological studies have relied on concepts from modern fire investigation to reconstruct ancient fires. As seen from the survey below, this approach has led to successful reconstruction of fires only in cases of exceptional preservation or over small excavation areas.

The study of fire behaviour is a well-established discipline revolving around several main foci: prevention of fires, recommended actions during fires, construction of fire-resistant structures and the investigation of fires that have occurred (Quintiere, 1998; 2006; DiNenno et al., 2002; Christensen and Icove, 2004; Chandler, 2009; Lentini, 2013; De Haan and Icove, 2014). The basic scientific approach to fire investigation is a systematic study of the scene and the collection of evidence very similar in some aspects to an archaeological excavation (Icove et al., 2013; 2014). The evidence is then examined in the light of models from fire engineering and fire dynamics studies (De Haan and Icove, 2014: 17).

Applying the modern knowledge to archaeological cases is not straightforward, mainly because in archaeology the examination of the scene takes place hundreds or thousands of years after the conflagration event. It is therefore to be expected that the evidence at the archaeological site has been altered by later activities (e.g., reclamation of artefacts, construction) as well as weathering.

Another challenge is that ancient fires differ from modern ones in their materiality, namely in the nature of construction materials and their transformation during conflagration (Icove et al., 2006: 12;

Alperson-Afil, 2012). Most modern structures employ concrete, plastic, various metals and complex materials in their construction, while Neolithic to Iron Age structures were built from stone, sun-dried mud bricks, wattle-and-daub, and wood and other types of vegetal matter. Similarly, items stored in structures are made of different materials in different periods, with modern materials being known to release energy much faster than legacy materials and thus facilitate a more rapid growth of fire (Kerber, 2012). Likewise, heat is conducted at different rates in different solids (Rockett and Milke, 2002), and thus the same fire might have different effects in differently built structures. Furthermore, electrical wires and appliances, among the most common sources of modern fires, are not relevant to the past, while modern structures include mechanisms (i.e., fire suppression systems, fire-fighters) to ameliorate the effects of fires. The vast majority of studies in modern fire investigation consider only modern materials, construction techniques and architecture, and therefore require adaptation so they can be applied to ancient cases.

Some studies attempting to understand ancient fires did not emphasize the above-mentioned dissimilarities. For instance, micro- or macro-archaeological tools were used to determine temperatures, but the reconstructions of ancient fires were not based on insights from fire investigation (Shoval et al., 1989; Puytison-Lagarce and Lagarce, 2006). Stevanović (1997) employed concepts from modern fire investigation, but they were outdated (based on a source from 1969). Consequently, she identified the locations of ignition only on the basis of specific locations where the highest temperatures were reached, and wrongly assumed that high temperatures (in the range of 700–1000 °C) are indicative of arson (Stevanović, 1997: 375–376, 381). Cunningham (2007: 36–39) noted molten pottery across a building in Palaikastro (Crete) and interpreted this observation using concepts from fire investigation to infer that a flashover had occurred, yet in this case the fire propagation path and fire origin was not determined. At Çatalhöyük, the excavators used visual observations such as soot marks on walls and changes in the colours and hardness of floors, and interpreted these observations in the light of concepts from fire investigation such as the availability of oxygen during fire and the formation of soot patterns (these concepts are described below) to identify the location of ignition and to reconstruct the general progress of fire (Harrison, 2008; Twiss et al., 2008). Nevertheless, micro-geoarchaeology was not integrated in those studies, and therefore layers of debris on the floors received little attention and the fire temperatures were surmised rather than reconstructed based on empirical data. Furthermore, while concepts from modern fire investigation were used in these studies, they were based on exceptional preservation of soot and scorch marks on intact plastered walls, which are rarely found in other sites. Consequently, the approach used at Çatalhöyük is not applicable to most other Near Eastern sites.

1.4. State of research: Experimental archaeology

An important step towards the integration of concepts from modern fire investigation in archaeological study of ancient fires came in the form of experimental studies. Several studies have examined fire and collapse of structures built either solely from combustible matter (e.g., wood, thatch) or with roofs made of organic matter (Bankoff and Winter, 1979; Friede and Steel, 1980; Christensen et al., 2007; Tipper, 2012; Gheorghiu, 2016). Broadly speaking, in the ancient Near East houses were rarely built in such a way, and thus these studies are of lesser relevance for the current study. Icove et al. (2006) and Lally and Vonarx (2011) investigated the distribution of temperatures and effects on structures of relatively short (15 min), internally set fires. Kreimerman and Shahack-Gross (2019) conducted a series of experiments aiming at understanding the mechanism behind conflagration of mud-brick structures. To do so they examined the effect on walls, roofs and floors of experimentally built replicas of mud-brick structures in four scenarios: (1) ignition of an uncovered vegetal roof; (2) ignition of a vegetal roof covered by mud plaster (3); ignition on the floor of a room covered by a mud-plastered vegetal roof; (4) ignition on the floor of a room covered by a mud-plastered vegetal roof and containing a vessel filled with olive oil. Their results include micro-geoarchaeological data and macroscopic observations from vertical and horizontal wall cross-sections that accord with knowledge from modern fire investigation and can be used to understanding conflagration in archaeological mud-brick structures.

1.5. Integrating fire investigation with micro-geoarchaeology, experimental and field archaeology

As can be seen from the above survey, the main gap in our knowledge is how to apply concepts from fire investigation and experimental studies to commonly found archaeological evidence. Below we focus on theoretical aspects of two important fire investigation parameters that are commonly present at archaeological sites and can be identified using micro-geoarchaeological tools: (1) spatial and stratigraphic distribution of heat retrieved from sediments, mud bricks and wall segments, and (2) spatial and stratigraphic positions of ash, charred material and soot.

1.5.1. Distribution of heat

As was shown in Section 1.2, it is possible to map the temperatures to which sediments were exposed across a structure using FTIR spectroscopy. In order to interpret such temperature maps it is vital to understand the mechanisms that underlie fire dynamics and thus heating of mud bricks, walls, roofs and floors during compartment fires, i.e. fires in closed spaces. This section describes in brief these mechanisms and offers concepts for interpreting temperature maps (Fig. 1a). Roof architecture is important for understanding fire dynamics. When the roof is made of vegetal matter it might easily ignite, collapse rapidly and serve as a major fuel source during the conflagration (Christensen et al., 2007; Tipper, 2012; Kreimerman and Shahack-Gross, 2019: 2918). On the other hand, when the roof is covered by mud, or another fire-resistant material, it will not ignite easily and will in fact promote the accumulation of a layer of hot gases below it for a relatively long time (Gordon, 1953; Icove et al., 2006; Kreimerman and Shahack-Gross, 2019: 2918–2919). As structures in the Bronze and Iron Age Near East are built in the latter way (Wright, 1985; Reich, 1992), we focus our discussion below on mud-brick architecture with this type of roofing.

For ancient compartments, most combustibles of animal and vegetal origin fall in the category of hydrocarbon fuels having a fluctuating flame temperature of about 800 ± 300 °C (Quintiere, 1998: 144–145). Yet despite the flame temperature of various fuels being roughly the same, we see significant variability of the maximal temperatures to which sediments were exposed in ancient compartment fires, ranging from 500 °C (and possibly less) to approximately 1200 °C (e.g., Shoval et al., 1989; Stevanović, 1997; Namdar et al., 2011; Regev et al., 2015; Faust et al., 2017). This stems from the fact that the air temperature of a compartment during fire depends primarily on the energy generated by the fire per unit of time (known as the Heat Release Rate, hereafter HRR) and on ventilation. HRR depends mainly on the amount of combustible materials burning at the same time (Walton and Thomas, 2002).

Heat transfer in fire is a widely discussed topic. Here, only four archaeologically relevant points are emphasized. From here on, when referring to high temperatures we mean >500 °C and when referring to low temperatures we mean < 500 °C, as these temperature ranges are based on estimates that can be obtained from the infrared spectrum of clay minerals. First, most of the heat generated by a fire plume is normally the convective flux that is carried away above the flame (Heskestad, 2002: 2.2). In closed compartments, most of the gases released are trapped together with the convected heat close to the ceiling and spread across it. Consequently, the compartment includes two distinct thermal layers – a hotter upper layer consisting of combustion products and a colder lower layer of air. As the fire continues, the upper layer becomes hotter and thicker (Quintiere, 2006: 340–341). This explains the observations made experimentally by Kreimerman and

Shahack-Gross (2019), namely that in mud-brick structures the upper courses of mud-brick walls and the mud roofs are exposed to higher temperatures than the lower courses and the floor.

Second, during compartment fire, the hot gas layer next to the ceiling expands through openings to other rooms. The farther these hot gases travel away from the source of burning, the more they come into contact with cooler air and their temperature decreases (De Haan and Icove, 2014: 71). Consequently, it is possible that even in rooms where flaming fire does not occur, the upper courses of walls will be exposed to high temperatures as a result of interaction with such an expanding hot gas layer.

Third, as mentioned above, the hot gas layer in a room may become hotter and thicker as the fire progresses. In some, although not all, cases this layer may become hot enough to ignite in a rapid reaction known as flashover. From this point, the fire enters the fully-developed stage, namely when all the combustibles in a room are involved and the size of the fire is dictated by the amount of air (oxygen) available through ventilation openings. Such a fire normally reaches temperatures in the range of 700–1200 °C (Quintiere, 2006: 340–342). It should be noted that a fully-developed stage can be reached after gradual fire growth with no preceding flashover. Thus, the best explanation for high temperatures across a room is a fire that has reached the fully-developed stage.

Fourth, if a fire does not reach a fully-developed stage, floors may be exposed to high temperatures only if they come in contact with burning objects. When a compartment fire reaches a fully-developed stage, the burning gas layer will usually radiate heat to the floor, which will be evenly heated. Therefore, areas of high temperatures across an entire floor are best explained by a fully-developed fire (Quintiere, 2006: 340–342; Lentini, 2013: 68–75).

Based on the above, the following heat patterns are expected to remain after conflagration at archaeological sites built primarily from sun-dried mud bricks (Fig. 1a): the highest temperatures will be found at the upper parts of walls and the roofs; walls heated from only one side (such as external walls) will show a temperature gradient due to heat diffusion and loss to the outside environment (see example in Kreimerman and Shahack-Gross, 2019: Figs. 9–11); and walls heated from all directions (internal walls) may show a symmetrical gradient if the fire was of short duration or may be burned throughout their volumes if the fire's duration was long enough (Kreimerman and Shahack-Gross, 2019). Floors will show meagre signs of heat (exposure to high temperature being limited to small areas across the floor) if the fire did not reach a fully-developed stage, and will show extensive burning (large areas of the floor being exposed to high temperatures) if the fire reached a fully developed stage. In the case of prolonged abandonment and/or demolition of a burnt structure in preparation for reconstruction, the following stratigraphic sequence is expected to form: floor (with meagre or extensive signs of heat), overlain by ash and charcoal from combustibles, overlain by collapse of mud-covered roofs and upper courses of mud-brick walls characterized by exposure to high temperatures, overlain by collapse/weathering products of mud bricks from the lower parts of walls characterized by exposure to lower temperatures. These heat patterns can be identified through the interpretation of infrared spectra of clay and other minerals, across space and along stratigraphic sequences at any archaeological site constructed from sun-dried mud bricks and wooden beams that have undergone destruction by fire (Fig. 2).

1.5.2. Ash, soot and charcoal

Wood and other cellulosic materials burn not directly but through a process of pyrolysis, i.e., the breaking of a substance into molecules through heat and the production of volatile gases and charred matter (Braadbaart and Poole, 2008: 2435; De Haan and Icove, 2014: 133). The hot gases react with oxygen in the air, a reaction visible by the flame above the fuel source (the height of the flame is proportional to the amount of gases released).

Charred matter is combustible as well, but its burning process is a very different one known as smouldering. Here the combustion is directly that of the char reacting with oxygen on its surface. It is a slow, low-temperature, flameless process, self-sustained by the heat evolved (Ohlemiller, 2002: 2.200). If the smouldering process continues for long enough, at the end of the process all that is left is ash — an inorganic grey to whitish fine-grained material. If, on the other hand, the smouldering process is incomplete, some charcoal is left. The smouldering process will normally continue much longer than flaming combustion and can last for several hours after the cessation of the flames (Braadbaart and Poole, 2008: 2435–2436). One of the main reasons for carbonization is limited oxygen, due either to physical barrier (e.g., no air circulation) or to short combustion time. For the purposes of archaeological interpretation, if a room presents a thick layer of ash on its floor, it follows that organic matter present in the structure before burning (e.g., roofing, matting, bedding, furniture, food, and more) was completely consumed, while large quantities of charcoal indicate that the combustion was not complete.

Soot is a solid powdery residue formed by incomplete combustion of carbon-based fuels (De Haan and Icove, 2014: 5). Soot patterns may appear on walls, ceilings and floors, and are often found next to openings such as doors and windows. Fire soot patterns have been discussed in detail (e.g., Chandler, 2009: 261–294; Harrison, 2013; Lentini, 2013: 76–124), and here only two archaeologically relevant patterns are briefly discussed. The best-known examples of soot patterns are those found on walls adjacent to the fire source. A fire with low HRR will leave an inverted V-shaped pattern (Lentini, 2013: fig. 3.12), whereas a fire with higher HRR will leave a V-shaped pattern (Harrison, 2013: Fig. 5). Soot patterns may also occur on the upper part of openings where hot gases escape a room, thus indicating the direction of fire development (Chandler, 2009: 269; Lentini, 2013: 77).

Fig. 1 presents a model that summarizes the types of evidence that are instrumental in the investigation and reconstruction of the course of fire at archaeological sites. As these patterns are produced by well-established physical processes, and are identifiable by using both field observations and micro-geoarchaeological data, they can be used to recreate the fire's development (De Haan and Icove, 2014: 259–260, 267–313). Following these patterns in the reverse direction to the development of fire will lead the archaeologist to identify the localities where fire burned for longer than in other places. All other factors, including fuel load and ventilation, being equal, these localities correspond to fire's origin (De Haan and Icove, 2014: 268). Areas of fire origin, in ideal conditions, are thus characterized by deeper heat penetration into surfaces and more extensive overall damage.

When fuel load and ventilation are not uniform, or are unknown as in the archaeological case, the location where fire burned for the longest time does not necessarily correspond to the exact point where fire started. Yet, when fire started outside of the area where it burned for the longest time, it usually still had enough time to burn in oxidizing conditions and to expand to other areas. Therefore, the place of origin is still expected to be relatively rich in ash, while places where only charred material is found could generally be ruled out as potential areas of origin. Possible indicators of the area of origin, especially in pre-flashover conditions, could be in the form of localized heating on the floor or indicative soot patterns on the walls (Fig. 1).

The National Fire Protection Association (NFPA) Guide for Fire and Explosion Investigations (NFPA 921, 921.221) stresses that finding the area of fire origin is not enough for determining the cause, whether arson or accident. For archaeological cases the best direct evidence for intentional arson is the identification of multiple ignition sources (e.g., Twiss et al., 2008). It should be noted, however, that a single ignition source does not preclude an intentionally set fire.

Below we present a case study of destruction by fire of a structure — a Near Eastern Bronze Age temple. The structure, known as the North-East Temple at Tel Lachish, occupied an area of approximately 300 m^2. Our study examines the destruction of this temple using the

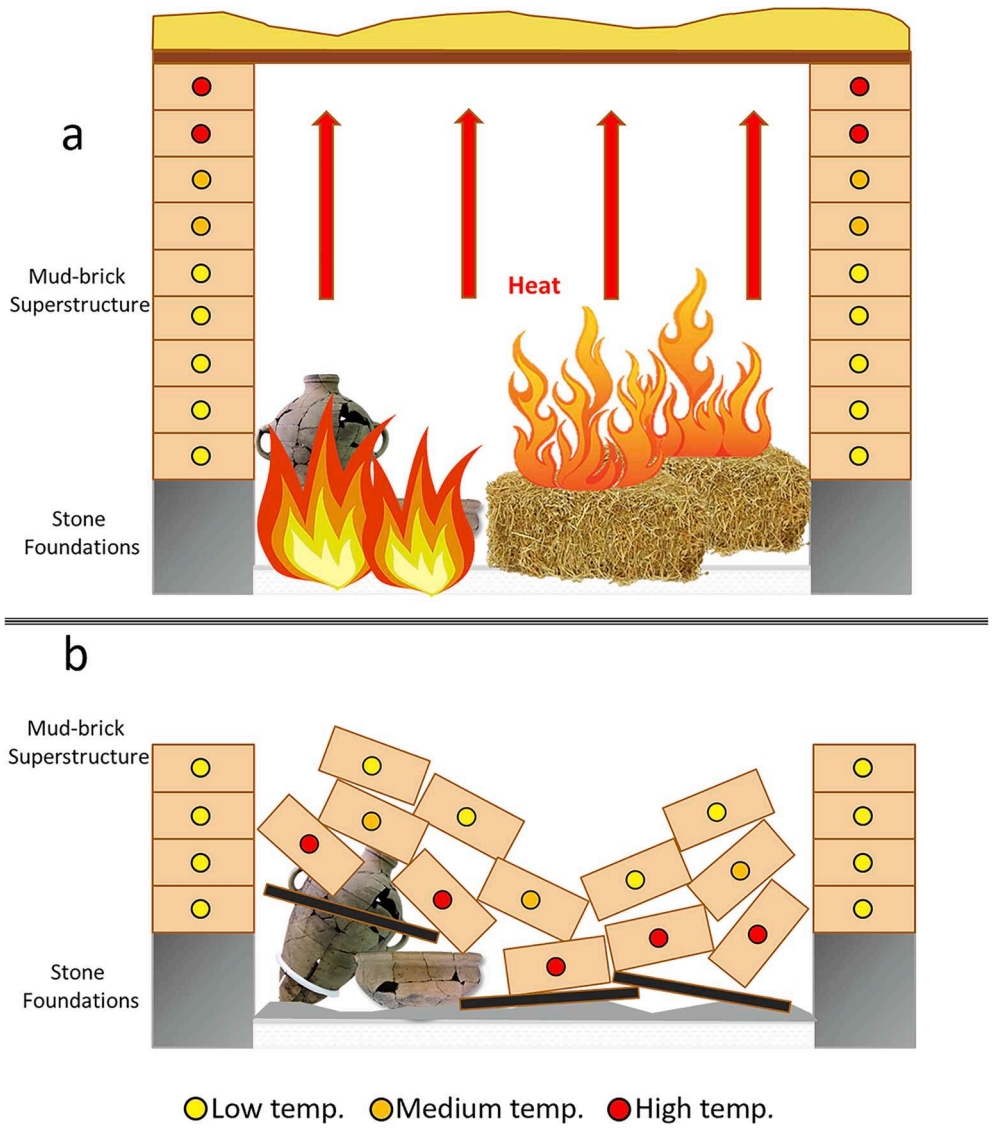

Fig. 2. Schematic model of fire and collapse of a single-storey mud-brick structure. (a) During combustion in a compartment, temperatures are higher at the top of the structure and the upper courses of mud-brick walls are exposed to the highest temperatures, while the lower courses of the same walls are exposed to lower temperatures. The upper parts of walls and ceiling may break up and collapse during the fire; these are expected to be burned at the highest temperatures within the compartment, and they accumulate directly on the compartment's floor. (b) After the fire event, mud-brick walls may further deteriorate or be knocked down intentionally (e.g., for purposes of rebuilding). As either deterioration or knocking down will remove upper wall courses first, these processes will result in further accumulation of highly fired brick wall courses close to the floor level, followed by accumulation of the middle and lower brick wall courses. The expected eventual stratigraphic sequence includes a floor level with no or few signs of high temperature, a lower debris level with many signs of high temperatures, and an upper debris level with signs of less intensive temperatures.

integrative interpretational framework presented above, combining stratigraphy, micro-geoarchaeology and fire investigation. We note that such reconstructions will be best where large areas of a destruction level have been exposed (at least several tens of square metres) and will be less meaningful where small exposures of destruction are studied.

2. The North-East Temple at Tel Lachish

2.1. Level VI at Lachish – Background

Tel Lachish is a prominent archaeological mound in the Shephelah region in southern Israel, occupied from the Neolithic to the Hellenistic period. Level VI at the site represents the last Canaanite city, known from previous excavations to have been destroyed by fire (Ussishkin, 2004a: 71–72). The time of this destruction was recently determined by a Bayesian model of radiocarbon dates to be 1210–1126 BCE (95.4 % range; Garfinkel et al., 2019a).

The cause of the city's destruction has been debated. Most scholars have assumed that the destruction of Level VI resulted from conflict and tried to identify the destroyer based on historical considerations (e.g., Albright, 1935; Tufnell, 1953: 51; Ussishkin, 2004a: 71–72). Recently, Cline (2014: 121) noted the presence of several skeletons in the destruction debris (see below) and the absence of weapons, and suggested that the site could have been destroyed by an earthquake, while noting that no other evidence of earthquake was observed. Millek (2017: 128–131), on the other hand, also noted the absence of evidence of battle and has suggested that the main temple of the city (the Acropolis Temple, Area P) was first abandoned and destroyed, and that some time later a different building (the Pillared Structure, Area S) suffered an accidental fire that buried the inhabitants, presenting an interpretation of gradual abandonment (see Fig. 3 for the location of the structures; their abandonment and destruction processes are discussed below). Regrettably, none of the cited evidence could point unequivocally at the cause of destruction. As mentioned above (Section 1.1), skeletons buried in the destruction debris are not unique to earthquakes, and the absence of weapons in the destruction debris cannot be used as evidence that a site was not destroyed as a result of conflict. Therefore, in order to identify the ultimate cause of Lachish VI's destruction it is necessary to understand whether conflagration at the site was intentionally set or resulted from an accident or natural disaster. To address this question we focus on evidence of conflagration around the site. We first examine in detail evidence found in a recently excavated structure – the North-East Temple – and later integrate the results with data collected in older excavations.

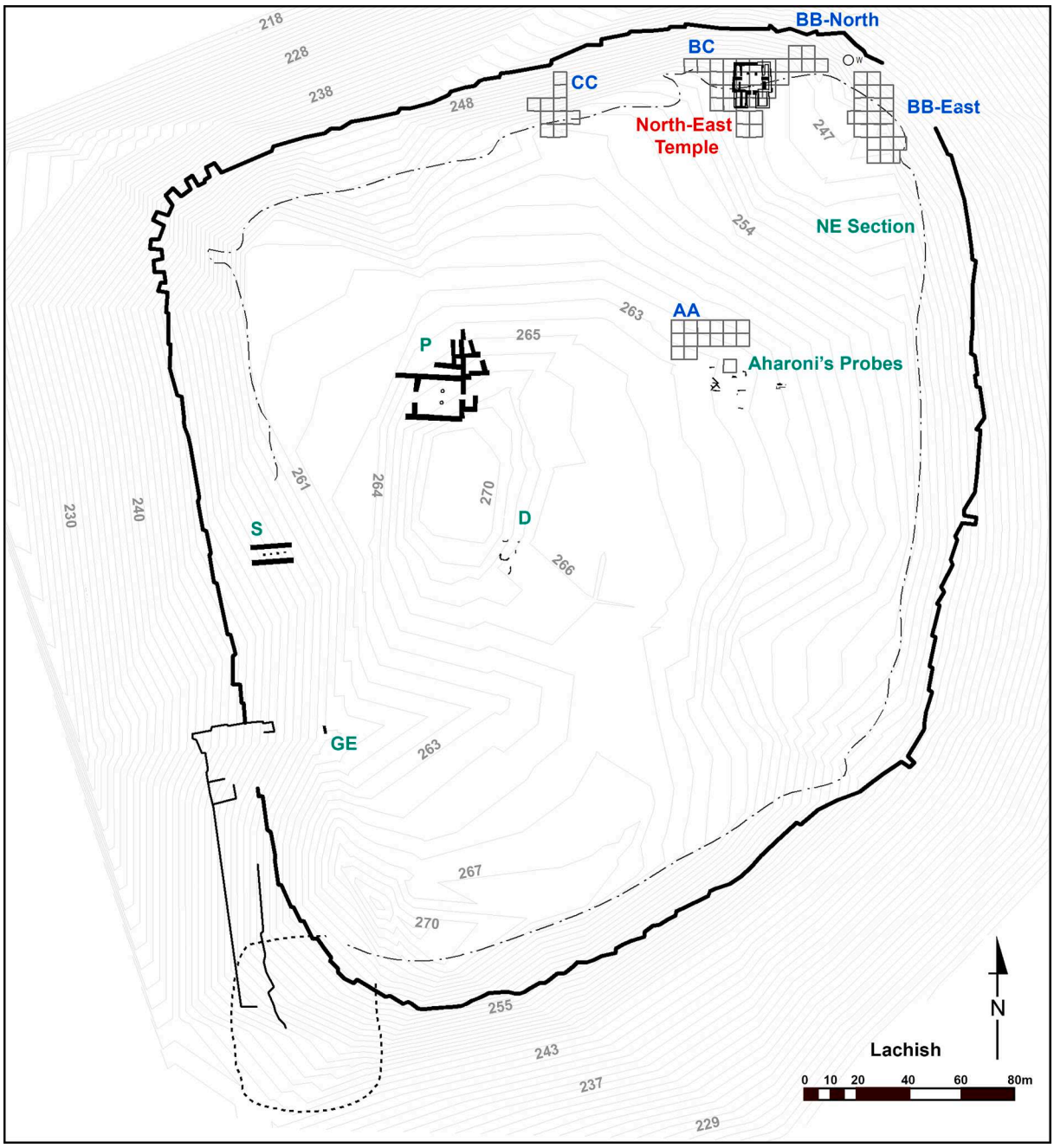

Fig. 3. Plan of Tel Lachish showing principal remains of Level VI excavated by all expeditions. Areas excavated by the Fourth Expedition to Lachish are marked by blue letters and grey excavation squares. Areas excavated by previous expeditions are marked by green letters (based on a drawing by D. Perez). (For interpretation of the references to colour in this figure legend, the reader is referred to the web version of this article.)

2.2. The North-East Temple

The Fourth Expedition to Lachish (2013–2017), a joint project of the Hebrew University of Jerusalem and Southern Adventist University (Garfinkel et al., 2021), exposed a large structure currently understood to be a temple belonging to Level VI, dubbed the North-East Temple (hereafter NET) (Weissbein et al., 2019). The NET is located in Area BB, in the north-east corner of the site (Fig. 3). In the western side of the area, the upper part of Level VI was found directly below topsoil (ca. 20 cm below the current surface), while its floor was found about 1.4 m below; the walls were preserved to a height of approximately 1.2 m. The eastern side of the same level has been affected by erosion, so that only the foundations of walls were preserved and the accumulation above the Level VI floor was no more than 20 cm thick. The floor in the eastern part was therefore less well-defined than in the western part of the area. Wall foundations made of local field stones provided an architectural picture of a single large structure (Fig. 4).

2.2.1. Architecture, construction materials and techniques

The structure is 19 m long and 16 m wide, covering an area of ca. 300 m2. It was oriented on a north–south axis and entered from the south. On the basis of architectural parallels and material culture finds, it is identified as a 'Syrian Temple' or 'Tower Temple' (Fig. 4; Mazar, 1992: 164–173; Weissbein et al., 2019). It consists of eight architectural units (A–H; Fig. 4): an entrance portico (Unit A) flanked by two towers (Units B–C), a main hall (Unit D), two rooms to the west of the main hall

(Units E–F), at least one more room to the east (Unit G), and another room, which probably served as the holy of holies, to the north of the main hall (Unit H).

The NET's construction was typical of the Near East. The walls were composed of a stone foundation (ca. 0.9 m high) and a mud-brick superstructure. The walls were probably not plastered by lime, as no remains of this material were found in the debris. Remains of charred wood and roof fragments – pieces of burned clay with reed impressions that represent the remains of a layer of mud that covered the roof – were found wherever preservation was good, suggesting that most of the architectural units were roofed. There was no indication of a second floor. Overall, it seems that the NET was a single-storey sun-dried mud-brick structure with a mud-plastered vegetal roof.

2.2.2. Phases of occupation, crisis and abandonment

Material culture finds that support the identification of this structure as a temple include two standing stones (Inst. BB1132), two bronze 'smiting god' figurines and a bronze sceptre plated with silver in Unit D, two deposits of large bronze cauldrons (one in Unit D and another at the entrance to Unit E) and a deposit of jewellery and metal objects in the northern wall of the temple, Wall BB262 (Weissbein et al., 2019; Garfinkel, 2020; Fig. 4).

The two superimposed floors in the main hall (Unit D) indicate that the temple has two stratigraphic phases. The earlier phase is represented by the units described above, the metal and jewellery foundation deposits, and scant finds mainly in the form of pottery sherds and bones. This phase does not show any evidence of destruction. The second phase is composed of the addition of Wall BB1165, which partitions the southern part of the main hall (Unit D), an oven (Inst. BB1193; Fig. 4) and a storage installation (Inst. BB1067). Wall BB1165 was evidently not straight, built of stones of varying sizes and of inferior construction quality, and does not follow precisely the main axis of the temple. Inst. BB1067 is crudely constructed and blocks the main axis of the temple. Construction of inferior quality, obstruction of visual axes and the fact that a storage installation was built in the main hall of the temple fit Driessen's definition of 'crisis architecture' (1995; and see Section 1.1 above) and might indicate that the temple experienced decline in its last days. Alternatively, these feature could represent a re-occupation of an abandoned temple by squatters.

The pottery assemblage of the later phase supports similar interpretations, as it attests to domestic activities (mainly cooking and storage) that took place alongside the cultic activity (represented by the standing stones, the two 'smiting god' figurines and the bronze sceptre) (Weissbein et al., 2019). Unit E was the only architectural unit that yielded almost no pottery but large quantities of carbonized grain and ash. Carbonized grain was also found in storage jars in the north of Unit F.

To summarize, because evidence for domestic activities in a temple is unusual, and as this phase is also accompanied by 'crisis architecture' the later phase probably reflects either a social crisis (Driessen, 1995; Zuckerman, 2007; Weissbein et al., 2019) or a total abandonment of the temple and a re-occupation by squatters. We prefer the former interpretation because of evidence of cultic activity in the structure's last phase that includes portable objects of cultic nature, such as bronze 'smiting god' figurines, a bronze sceptre and a silver pendant, that would have been removed if the structure was abandoned altogether and later reused solely for residential purposes.

As mentioned in Section 1.1, models for the study of abandonment behaviour have generally demonstrated that the more *de facto refuse* (as defined by Schiffer 1987: 89; see Section 1.1), in our case meaning abandoned items, is found in a structure, the faster was its abandonment (LaMotta and Schiffer, 1999). The assemblage of finds in the NET is rich and includes numerous pottery vessels of many sizes and types, organic commodities such as grain, metal objects and some jewellery. Consequently, it seems that the NET was abandoned rapidly.

2.2.3. Post-destruction activities

After the temple's destruction and the collapse of its walls the area was left unoccupied, with no structure being constructed over the debris, for at least 150 years, until the building of Level V (Garfinkel et al., 2019a). The only activity that can be associated with this time frame is a pit dug into the destruction debris in which a lamp-and-bowl deposit was placed (Weissbein et al., 2019). There is no evidence of pits dug to rescue trapped objects from the debris. The Level V remains were built on top of the debris of Level VI, approximately 1.2 m above the Level VI floor, and could have removed the uppermost part of the Level VI debris. No walls or foundation trenches of Level V penetrated deep into the debris and disturbed the objects or deposition sequence in the western part of the temple. As mentioned above, erosion did severely affect the eastern part of the temple.

Below we present the integrative research approach used in the study of the NET destruction.

3. Materials and methods used for the integrative case study

3.1. Sampling methods

An intact sun-dried mud brick from a Middle Bronze Age citadel at the site was collected as a control. The rationale for this was that it represents the local material used in antiquity for preparation of mud bricks and that it contains clays typical of the site's environs. After ascertaining (using FTIR spectroscopy; see below) that the clay component of this mud brick had not been heated above 450 °C, the brick was split into 5 sub-samples, each ca. 0.5 cm in diameter, which were heated in a laboratory furnace (Adam Mandel ©) to different target temperatures (500, 600, 700, 800 and 900 °C). In each cycle the oven's temperature was increased to the target temperature at a rate of 10°C/min and the oven was then kept at the target temperature for 2 h and left to cool down overnight. The variously heated brick sub-samples served to establish a calibration of the expected infrared spectra typical of heated mud bricks from Lachish (following Berna et al., 2007).

The location of ash, soot, burnt mud bricks, charred remains, restorable vessels, metal objects, jewellery and bone items was accurately recorded (to 5 cm accuracy) using triangulation and the elevation of each sample was determined to 1 cm accuracy by dumpy level. The focus of the study was on the western part of the temple, where a full stratigraphic sequence was preserved (Units D, E and F; Figs. 5, 6). Samples for mineralogical analysis geared towards identification of pyrogenic materials were collected from floor deposits, ash deposits, mud bricks (whole and fragmentary), and stones from wall foundations, as well as topsoil that served as control (totalling 177 samples; Table 2). About 50 % of large (more than 15 cm in diameter) mud-brick fragments were systematically sampled across the studied area. The samples were collected in a manner that insured random spatial distribution across all units (as far as possible). Samples were usually retrieved from fresh, clean brick surfaces and occasionally from brick interiors. In several cases we examined bricks in different spots, and the results were uniform. No heat gradient as observed by Kreimerman and Shahack-Gross (2019: 2922–2924) was found in any of the NET's mud bricks.

Sediments from excavation sections were sampled stratigraphically at the end of the excavation according to colour and texture differences. Sediments were sampled in bulk, with approximately 10–15 g of sediment being placed in plastic vials or plastic bags. Larger samples (20–50 g) were collected where concentrations of charred remains or powdery (possibly ash) deposits were encountered.

3.2. Laboratory methods

All samples were analysed using FTIR spectroscopy, utilizing the KBr method (Weiner, 2010: 275–278). A few micrograms of each sample were ground in an agate mortar and then mixed with tens of micrograms of KBr. The mixture was ground again and then pressed into a 7-mm

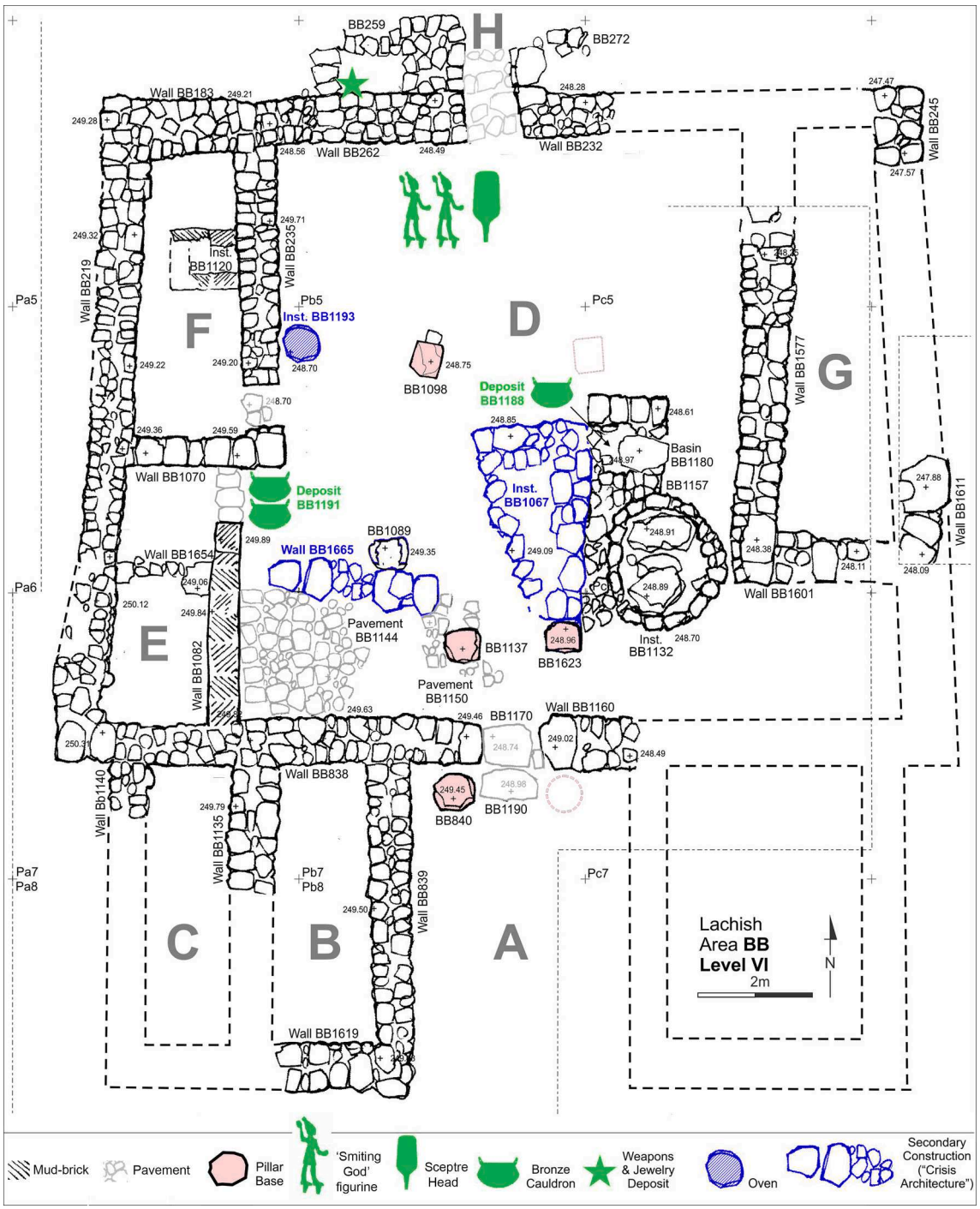

Fig. 4. Plan of the North-East Temple with the architectural units marked by bold grey letters A–H. Finds of special importance are in green and the second phase of construction ('crisis architecture') in blue (by J. Rosenberg). (For interpretation of the references to colour in this figure legend, the reader is referred to the web version of this article.)

pellet using a manual press (Specac). The pellet was placed in an FTIR Spectrometer (Thermo Scientific Nicolet iS5) and infrared spectra were obtained after 32 scans in the 4000–400 cm^{-1} spectral range using Omnic 9.3 software.

Heat intensity was determined from spectra, following the standard models that were presented in Section 1.2, by examining the absorbance bands that characterize clays (Berna et al., 2007; Forget et al., 2015), calcite (Regev et al., 2010) and aragonite (Toffolo and Boaretto, 2014). The results obtained were plotted on the top plan of the study area to allow appreciation of spatial heat patterns.

4. Results of the case study

4.1. Determination of heat regimes from experimentally heated local mud

Fig. 7 presents the spectra obtained from the heated mud-brick subsamples. Unheated material is composed of clay, quartz and calcite. Clay is evident in absorbance bands at 1034, 914, 525, 470, 3614 and 3696 cm^{-1}. Quartz is evidenced by strong absorbance at 1080 cm^{-1} associated with minor bands at 798–778, 695 and 1161 cm^{-1}. Finally, calcite is characterized by bands at 1431, 875 and 713 cm^{-1}. The lowest temperature that causes change in the spectrum of clay is 500 °C, as

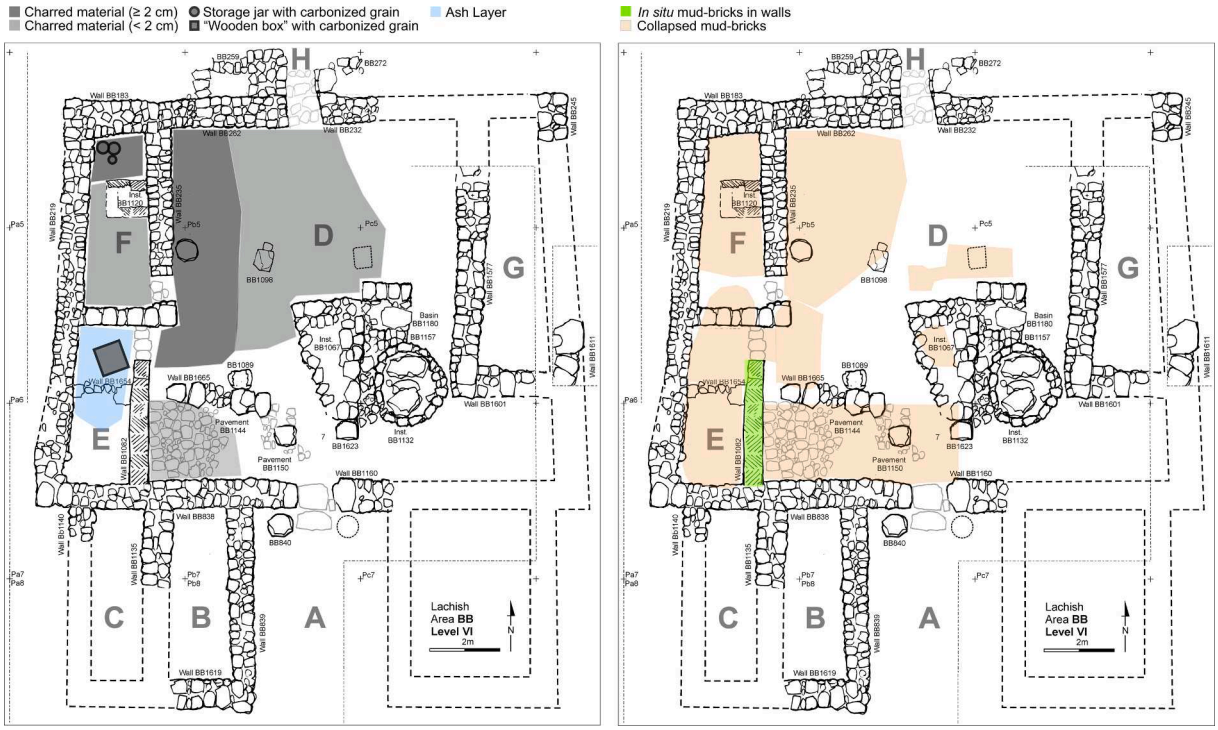

Fig. 5. Macroarchaeological evidence of destruction by fire (based on visual observations). (a) Location of ash and carbonized material typically found in the lowest part of destruction debris close to the floor level; (b) Location of *in situ* and collapsed mud bricks, the latter typically found overlying ash and charred remains (based on a plan by J. Rosenberg).

Fig. 6. Stratigraphic sequences typical of destruction by fire. **(a)** North-south section in Unit D (looking to the west) showing a grey-coloured compact floor (1) associated with stone installations and charred material, overlain by orange-coloured mud-brick debris (2). Scale bar is 1 m long. **(b)** Sequence in Unit E showing a charred layer (1) directly on the floor, overlain by ash (2) and mud-brick debris (3). Scale bar is 8 cm long (courtesy of the Fourth Expedition to Lachish). (For interpretation of the references to colour in this figure legend, the reader is referred to the web version of this article.)

Table 2
Samples subjected to FTIR analysis according to contexts and architectural units. Note that the locations of samples from lower collapse appear on Fig. 8 and those from upper collapse on Fig. 9. See the full list of samples in Table 3.

	Unit E	Unit F	Unit D
Floor	6	10	19
Lower collapse	18	9	26
Upper collapse	25	9	43
Walls	12		
Total	**61**	**28**	**88**

demonstrated by previous studies (e.g., Berna et al., 2007; Regev et al., 2015; Forget et al., 2015) and also seen in the controlled heating conducted here. The change is evidenced by the loss of absorbance bands at 3614 and 3696 cm^{-1} (i.e., structural water) and the disappearance of the OH deformation band at 914 cm^{-1} (Fig. 7). In addition, the major band of clay shifts from 1034 cm^{-1} to 1039 cm^{-1}. Following heating to 600 °C, a new band characteristic of calcium hydroxide appears at 3642 cm^{-1} due to calcite disintegration. As temperature increases, the height of the major band of clay (1035 cm^{-1}) relative to that of quartz (1080 cm^{-1}) decreases (indicting transformation into *meta*-clay; Shoval and Beck 2005; Shoval and Paz 2015). Below 600 °C the major quartz band is almost indistinguishable, while at 600 °C the 1080 cm^{-1} band forms a pronounced shoulder. At 700 °C or higher it is clearly seen as a separate band at 1080 cm^{-1}. Calcite disintegration continues at a temperature of 700 °C (the band at 713 cm^{-1} disappears, while the bands at 1430 cm^{-1} and 875 cm^{-1} become less pronounced). In samples heated to 800 °C the range from 1426 cm^{-1} to 1493 cm^{-1} appears as a flattened absorption band due to partial calcite decomposition also accompanied by broadening of the main absorbance band between 800 and 1100 cm^{-1}. The major band of quartz and *meta*-clay (1080 cm^{-1}) becomes more pronounced than that of heated clay (1040 cm^{-1}). In samples heated to 900 °C the band at 3640 cm^{-1} (calcium hydroxide) becomes less pronounced and a new band forms at 581 cm^{-1}, most probably an outcome

of the formation of a new, as yet unidentified, high-temperature mineral (possibly gehlenite; see Waiman-Barak et al., 2018). In sum, the mineralogical changes detected in this controlled calibration form a model that can be used to extrapolate the maximum temperature to which sediments and mud bricks have been exposed in the NET.

4.2. Evidence of destruction in the North-East Temple

Evidence of destruction is described here according to architectural units. The NET displayed a stratigraphic sequence typical of destruction in Near Eastern *tell* sites: a floor (either beaten earth or paved), overlain by a ca. 1–5 cm thick deposit of charred material (Fig. 6a) or a thicker layer of ash (Fig. 6b) that included pottery (much of it restorable), overlain by a 0.5–1 m thick layer of collapse debris containing orange-coloured mud bricks (mostly fragmented) and pottery.

Figs. 8 and 9 and Table 3 show the reconstruction of heat intensity as recorded by FTIR analysis according to elevation in the stratigraphic sequence. Floors in the temple are of two types: beaten earth and stone-paved. The exact surface of beaten-earth floors is difficult to identify in the field, while paved floors were presumably swept and did not accumulate sediment during activity in the temple. The southern part of Unit D includes a paved floor. Beaten-earth floor levels were deduced from the following: presence of a phytolith-rich ash layer (Unit E), presence of fallen mud bricks (all units), and presence of flat-lying pottery associated with a black layer, usually less than 5 cm thick (Units D north and F). None of the assumed beaten-earth floor samples showed exposure to temperatures above 500 °C (Table 3), and they are therefore not illustrated.

Fig. 8 includes samples found *above* the floor. For Unit E it includes samples from the phytolith-rich ash layer and from the 20 cm of sediment found above it, which includes the remains of a charred wooden box and several mud-brick fragments. Fig. 8 includes samples for Unit D-south from the sediment accumulation up to 20 cm above the paved floor and samples for Unit D-north and Unit F from the black layer lying on the beaten-earth floor.

The samples presented in Fig. 9 were collected at least 20 cm above the floor as defined above for each unit, and hence represent the upper part of the collapse debris. They include loose sediment as well as brick fragments.

Sediment and brick samples from the lower 20 cm of the sequence (Fig. 8) generally show high frequencies of exposure to temperatures of 500 °C and above (43 out of 50 samples; 86 %), while sediment and brick samples that were collected from the upper portions of the destruction sequence (Fig. 9) show this in lower frequencies (44 out of 77 samples; 57 %). This pattern is also evident in a sequence studied in Unit E (Fig. 10).

In addition, mud bricks that were found *in situ* on a wall foundation in Unit E (Wall BB) were heat altered at ca. 500 °C throughout their volumes (Fig. 5b; 3 bricks analysed, each tested in 4 internal locations; see Table 3).

In Unit E a rectangular black (charred) feature overlay grey ashes (see below) that were lying on the floor (Fig. 11). FTIR analysis of sediment samples from the grey layer demonstrated that this layer is dominated by opal and also includes aragonite and minor amounts of calcite and hydroxylapatite (Fig. 12). The origin of aragonite is most likely related to high-temperature combustion (Toffolo and Boaretto, 2014). Microscopic examination ascertained that the opal derives from grass phytoliths. The phosphate compound (hydroxylapatite) is probably a product of burning of phosphate-containing organic matter (Regev et al., 2010). Overall, it appears that this phytolith-rich ash layer was formed by combustion of large amounts of grass and some wood/bark. The rectangular feature, which measured ca. 0.9 × 0.9 × 0.15 m and included charred wooden beams and cereal grains, was interpreted as a wooden box that contained grain. A thick layer of orange-coloured mud-brick debris lay over and around this 'wooden box' and across all of Unit E. As mentioned above, this unit also included the only place where a mud-brick superstructure was found *in situ*, on the stone foundation of Wall BB1082.

Three samples from the stone wall in Unit E were analysed using FTIR spectroscopy. The results were plotted on a 'grinding curve' (as in Regev et al., 2010: Fig. 1). The best fit for the results was the grinding curve of 'modern lime plaster', implying that the stones of the partition wall underwent calcination at high temperature, probably in excess of 650 °C, and transformed to lime.

5. Interpretation and discussion of the case study results

In this section heat distribution patterns and the locations of ash, soot, charred matter and burnt bricks are interpreted in the light of the framework presented in Section 1.5 and Fig. 1, and a reconstruction of the fire in the NET is suggested.

5.1. Distribution of reconstructed temperatures in the North-East Temple

The model for vertical distribution of temperatures presented above (Section 1.5.1; Fig. 1a) states that bricks located in higher courses are expected to be exposed to higher temperatures during compartment fire than those in lower courses. When the building collapses, bricks from the uppermost courses are expected to fall directly on the floor and to be covered with bricks from lower courses. Consequently, mud bricks found lower in the collapse are expected to display exposure to higher temperatures than those found above them (Fig. 2). This model, also based on experimental studies (Kreimerman and Shahack-Gross, 2019), fits the case of the NET. Clearly, the lower 20 cm of the collapse are dominated by high-temperature debris (Fig. 8), while the deposits above are dominated by lower-temperature debris (Fig. 9).

The highest temperatures reconstructed in the NET (in Unit E) were in the range of 600–800 °C. As mentioned in Section 1.5.1, the best explanation for such temperatures across a room is a fire reaching a fully-developed stage, namely when all combustibles in the room burn simultaneously and the size of fire is dictated by the availability of oxygen. Notably, a fully-developed fire cannot be reached *after* roof collapse (i.e., choking of flames), and consequently the fire in Unit E carried on while the structure was still standing.

In Units D and F the reconstructed temperatures were mostly in the range of 500–600 °C. In the lower 20 cm of collapse most samples were exposed to these temperatures, while most of the deposits above were exposed to less than 500 °C. This means that when the structure was still standing only the upper courses in Units D and F were heated to above 500 °C. These observations suggest that only the upper parts of walls were exposed to high temperatures for a relatively long time and that Units D and F did not experience a fully-developed fire. The exposure to high temperatures at upper courses could be due either to localized fire in the room or to the expansion of a hot gas layer from adjacent rooms through openings (as described in Section 1.5.1).

5.2. Locations of ash, soot and charcoal in the North-East Temple

In the NET, Unit E is the only architectural space in which significant quantities of ash on the structure's floor. As mentioned in Section 1.5.2 (see also Fig. 1b) the presence of ash points to a prolonged fire under oxidizing conditions. This observation suggests that enough oxygen was present during the fire and therefore that it occurred while the structure was still standing (note that this conclusion is further supported by temperature maps; Section 5.1). The charred 'wooden box' feature was found within the ash, suggesting that it fell on and into hot ashes; i.e., either the wooden box and its grain contents were heated in reduced oxygen conditions or their combustion ended before they had the time to turn into ash.

The picture is different in Units D and F, where the floors are covered by carbonized fine matter including wood fragments and storage jars contain carbonized grains (Unit F), while ash was rarely observed. These

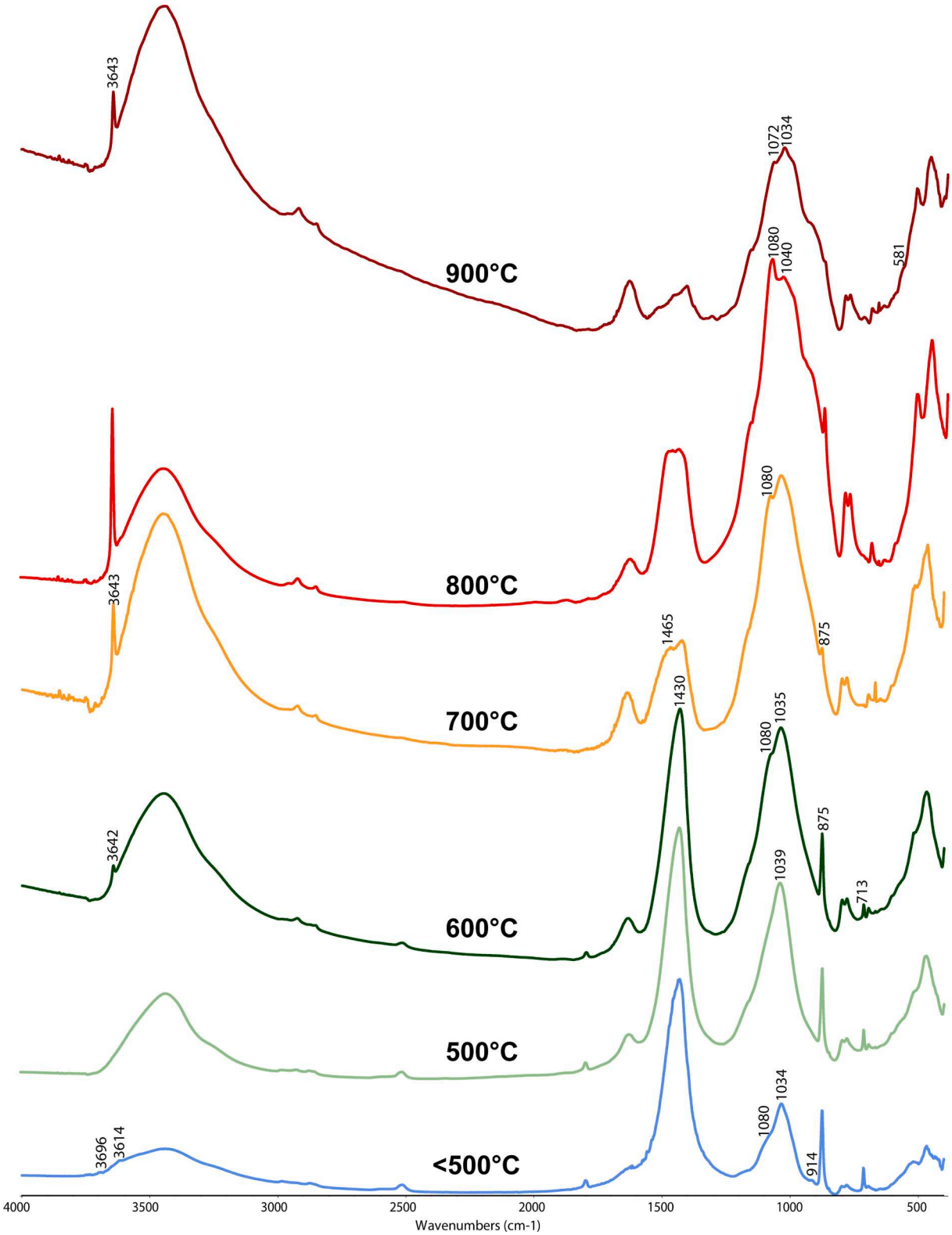

Fig. 7. FTIR spectra of experimentally heated sub-samples of an unheated mud brick from Middle Bronze Age Lachish. The lowest spectrum (<500 °C) is the unheated mud brick. The spectra above it show mineralogical changes with increased heating temperature. See text for details.

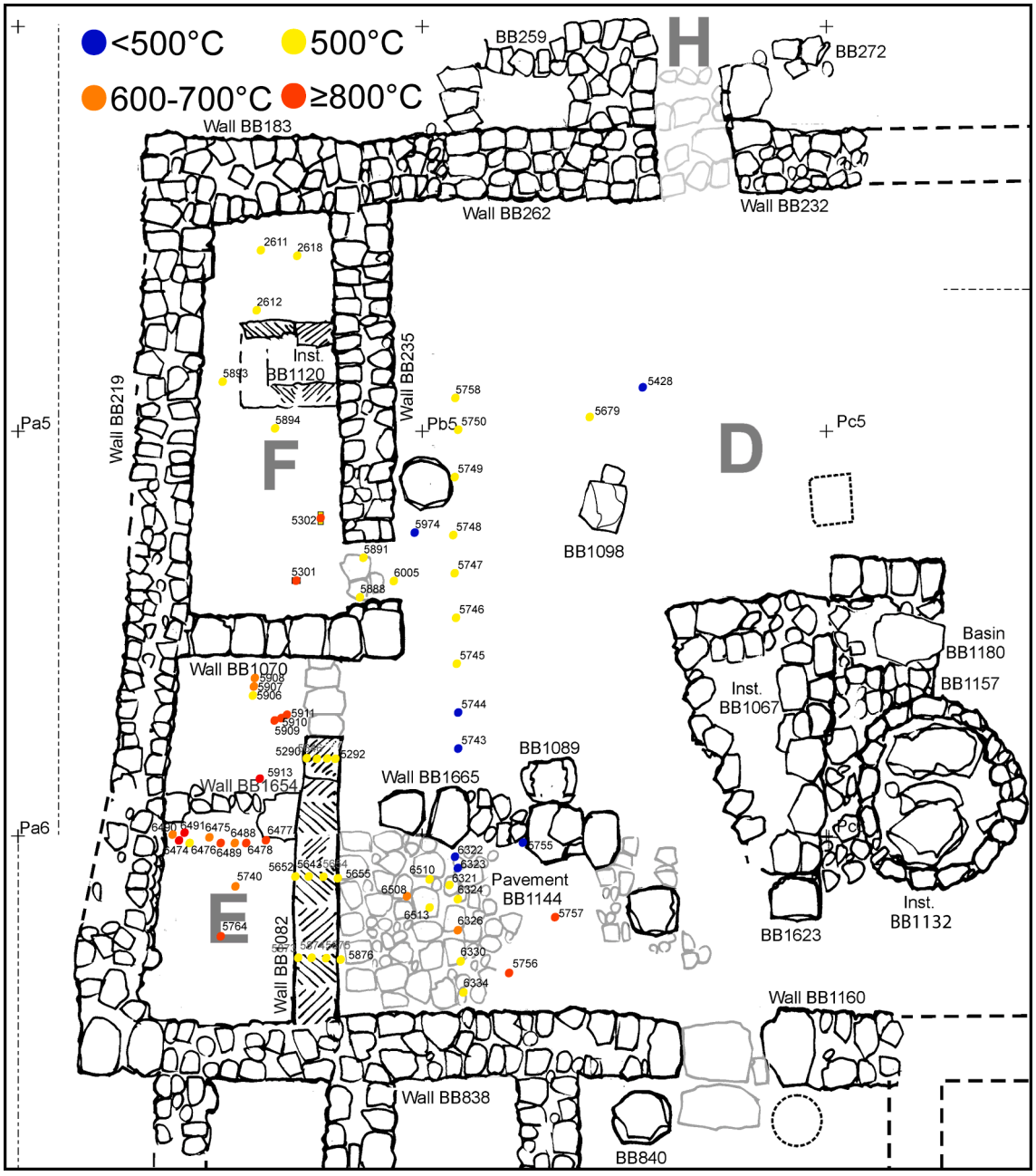

Fig. 8. Plan of the western part of the North-East Temple with locations of samples in the lower 20 cm of the destruction stratigraphic sequence and the temperatures to which they were exposed, reconstructed using FTIR analysis. Numbers indicate sample numbers.

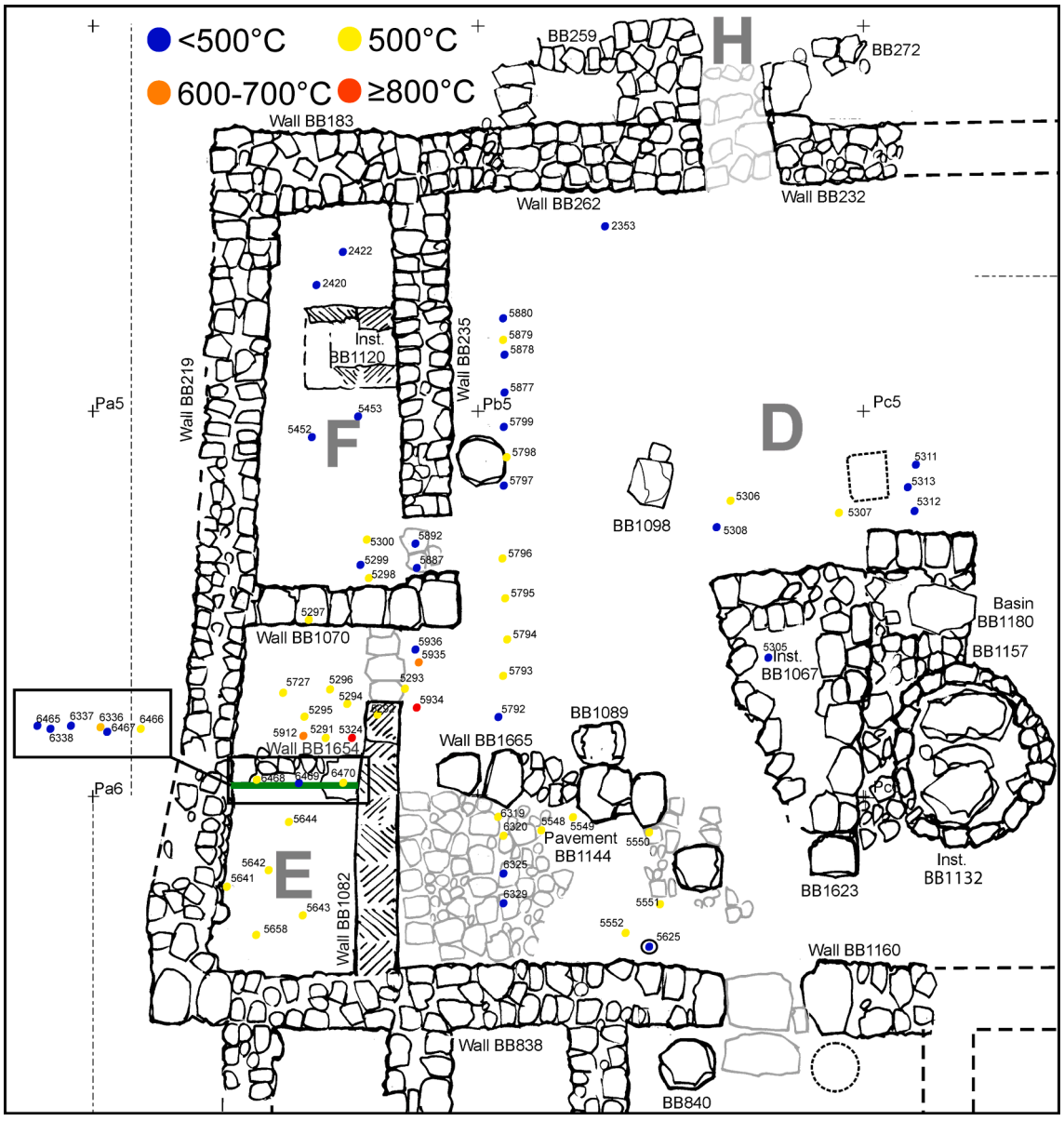

Fig. 9. Plan of the western part of the North-East Temple with locations of samples in the upper part of the destruction stratigraphic sequence (20 cm and more above the floor level) and the temperatures to which they were exposed, reconstructed using FTIR analysis. Numbers indicate sample numbers. The green line across Unit E marks the location of the section shown in Fig. 10. (For interpretation of the references to colour in this figure legend, the reader is referred to the web version of this article.)

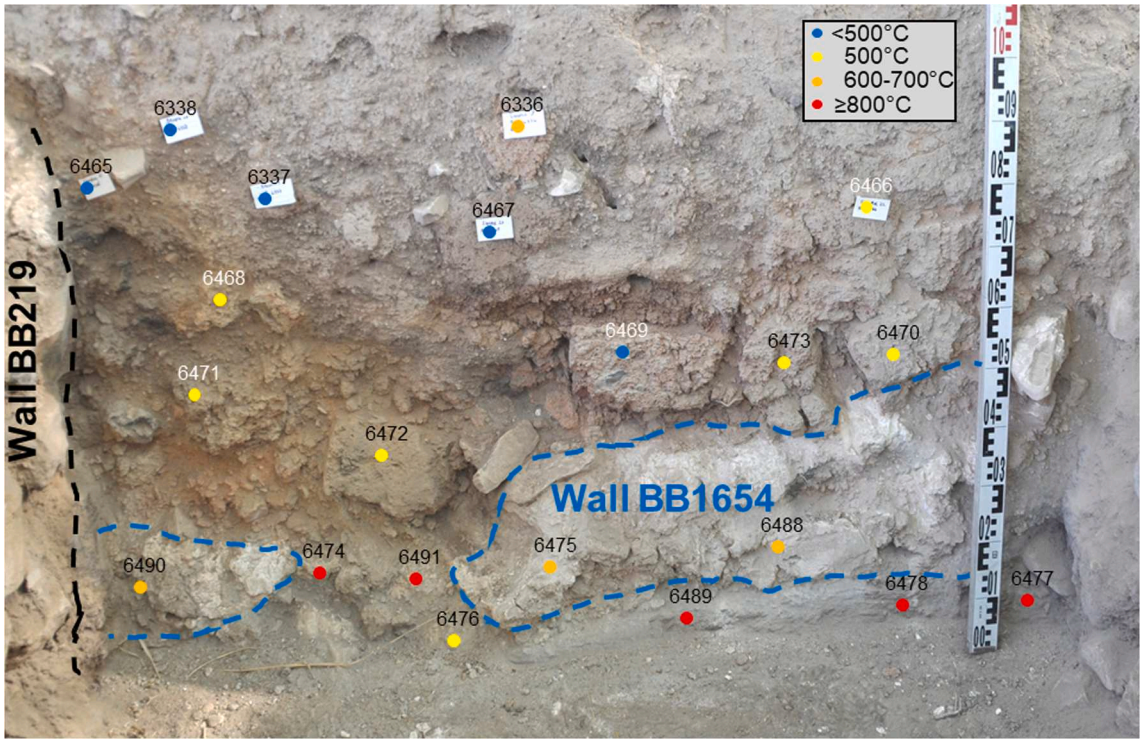

Fig. 10. East-west section through Unit E (looking to the south) showing position of samples studied (sediment, brick and wall stones; numbers indicate sample numbers), along with a colour-coded key to temperatures reconstructed using FTIR analysis. Note that the highest reconstructed temperatures are found at the bottom of this section (red dots; an ash layer), that the stones of Wall BB1654 have been calcined (samples 6475 and 6488), and that mud bricks in the lower level of the collapse were generally exposed to higher temperatures than those found in the upper part of the collapse debris. Note also that brick shapes were not preserved in the upper collapse because these bricks were exposed to temperatures lower than 500 °C and thus eroded into 'mud-brick material'. Section height from bottom of scale bar to top of photograph is 108 cm. (For interpretation of the references to colour in this figure legend, the reader is referred to the web version of this article.)

observations suggest that the fire in Units D and F was of short duration and/or oxygen-limited (Fig. 1b). Specifically, no locations on the floor where combustibles burned for a relatively long time could be observed.

Soot was found occasionally and in small quantities on walls. The lack of soot marks probably results from a lack of high-standing walls preserving their original faces. Consequently, no fire patterns on walls were observed.

5.3. Walls

For most walls, only the stone foundations were preserved; mud bricks were found *in situ* on stone foundations only in Wall BB1082. This is an internal wall between Units E and D in which the lower course of bricks is located 60 cm above the floor. These bricks were exposed to ca. 500 °C (Fig. 8; Table 3) and burnt through their volume. The presence of such a heat pattern of this wall strengthens the evidence for a prolonged high-temperature event (Fig. 1a) and supports its being an internal wall heated from all directions (cf. Kreimerman and Shahack-Gross, 2019).

5.4. Proposed reconstruction of the North-East Temple conflagration event

The reconstruction offered below is based on the better-preserved western portion of the temple. As no clear soot patterns were found, we attempt to identify the location of ignition where the fire had the longest time to burn.

The presence of a thick layer of ash and the high temperatures achieved in both low portions (calcined stones in wall foundations) and high portions (mud bricks) of Unit E show that a fully-developed fire occurred in this compartment of the temple. The remains of organic combustibles, found as a 15–20 cm layer of ash, suggest that the original grass and/or woody material was some 2–3 m high (extrapolated from experimental studies showing about 95 % volume loss of grass/wood matter upon full combustion; Shahack-Gross et al., 2005: 1421–1427). Considering this large amount of combustibles, it is reasonable to assume that the fire plumes were high and may have reached the roof. Yet the roof did not collapse immediately, as is evident from the fact that the combustibles turned into ash (i.e., oxygenated fire), a process that would not have been completed had the roof collapsed on partially combusted materials.

Heat forming close to the ceiling in the northern part of Unit E probably transferred across the partition wall to the southern part of Unit E and possibly escaped through the opening of Unit E into Units D and F.

Evidence for roof collapse at the end of the fully-developed fire in Unit E is found in the form of the charred wooden box that landed from above on and into the hot ashes; these are stratigraphically overlain by collapse of mud bricks. No charred roof beams were found (although occasional charred branches were present), but fragments of heat-altered clay plaster with reed impressions, probably representing mud plaster that covered the vegetal roof, were identified among the collapse debris. The reconstructed high temperatures, as well as the evidence for a large amount of organic combustibles, suggest that the northern part of Unit E was an area where ignition (primary or secondary) took place.

As previously mentioned, the stratigraphic sequence found in Unit F is as thick as the one in Unit E. It would therefore be expected to be preserved as well as the sequence in Unit E, yet it presents a very different picture. Ash is not found at the floor level, which is instead covered by charred matter, i.e., there is no evidence for a prolonged flaming fire in this room. The carbonization of grains found in storage jars placed on the room's floor indicates either lack of oxygen or a short duration of heat.

The stratigraphic sequence in the western part of Unit D is thinner than those in Units E and F. Here too there is no evidence for a thick ash layer, i.e., no evidence for a prolonged flaming fire, let alone one that

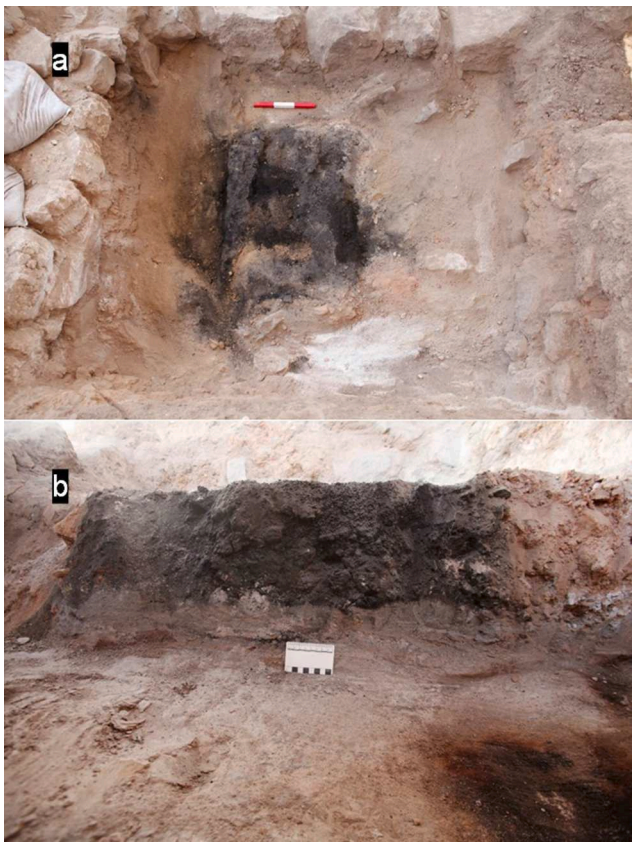

Fig. 11. The unique feature identified in Unit E. **(a)** The rectangular charred feature in oblique plan view (looking to the north). Note the charred wooden beam on the left. Scale bar is 30 cm long. **(b)** Section through the same feature (looking to the east). Note the well-defined boundaries of the feature and the fact that it sits directly on a grey ash layer and is surrounded by orange mud-brick debris. Scale bar is 8 cm long. (For interpretation of the references to colour in this figure legend, the reader is referred to the web version of this article.)

reached a fully-developed stage. Overall, the evidence in Units D and F suggests that ignition did not take place in these spaces.

It is difficult to explain the presence of burned-brick collapse in Units D and F, where there is no evidence for a prolonged fire. The following explanations may be considered: (a) ignition of chaff temper within bricks (as shown by Forget et al., 2015) in higher wall courses due to interaction with hot gases that expanded from Unit E; (b) burning of the roof in Unit D; and/or (c) post-conflagration dispersal of collapse debris, either naturally or by human agency, from the nearby Unit E. As some of the bricks and the charred matter in Units D and F were found as much as five metres away from Unit E (Fig. 5), it is less likely, to our mind, that mud bricks rolled so far away from their walls of origin after conflagration. We therefore prefer explanations (a) or (b). This interpretational uncertainty may serve as a lead for future experimental and archaeological research.

To summarize this section, ignition (primary or secondary) occurred in Unit E and the fire reached a fully-developed stage and was of relatively long duration. In Units F and D there is no evidence for ignition and the exposure to high temperatures was of relatively short duration.

5.5. Arson or accident – The North-East Temple and the demise of Level VI

In this study we have identified only one locality of ignition that developed into a flaming fire, in Unit E. Either arson or accident could have produced the evidence observed. We did not identify evidence such

Table 3
A Summary table of all samples used in the current study.

Sample	Source	Minerology	Temperature	Figure
Room F				
2420	Sediment	Clay, quartz, calcite	<500 °C	Fig. 9
2422	Sediment in jar	Clay, quartz, calcite	<500 °C	Fig. 9
2611	Sediment in jar	Clay, quartz, calcite	500 °C	Fig. 8
2612	Sediment	Clay, quartz, calcite	500 °C	Fig. 8
2618	Sediment	Clay, quartz, calcite	500 °C	Fig. 8
5298	Sediment	Clay, quartz, calcite	500 °C	Fig. 9
5299	Mud-brick	Clay, quartz, calcite	<500 °C	Fig. 9
5300	Mud-brick	Clay, quartz, calcite	500 °C	Fig. 9
5301	Mud-brick	Clay, quartz, calcite, aragonite	≥800 °C	Fig. 8
5302	Mud-brick	Clay, quartz, calcite, aragonite	≥800 °C	Fig. 8
5452	Mud-brick	Clay, quartz, calcite	<500 °C	Fig. 9
5453	Mud-brick	Clay, quartz, calcite	<500 °C	Fig. 9
5555	Floor (sediment)	Clay, quartz, calcite	<500 °C	
5556	Floor (sediment)	Clay, quartz, calcite (+charcoal)	<500 °C	
5715	Floor (sediment)	Clay, quartz, calcite	<500 °C	
5716	Floor (sediment)	Clay, quartz, calcite	<500 °C	
5717	Floor (sediment)	Clay, quartz, calcite	<500 °C	
5887	Sediment	Clay, quartz, calcite	<500 °C	Fig. 9
5888	Sediment	Clay, quartz, calcite	500 °C	Fig. 8
5889	Floor (sediment)	Clay, quartz, calcite	<500 °C	
5890	Floor (sediment)	Clay, quartz, calcite	<500 °C	
5891	Mud-brick	Clay, quartz, calcite	500 °C	Fig. 8
5892	Sediment	Clay, quartz, calcite	<500 °C	Fig. 9
5893	Sediment (debris)	Clay, quartz, calcite	500 °C	Fig. 8
5894	Sediment (debris)	Clay, quartz, calcite	500 °C	Fig. 8
5914	Floor (sediment)	Clay, quartz, calcite (+charcoal)	<500 °C	
5915	Floor (sediment)	Clay, quartz, calcite	<500 °C	
5916	Floor (sediment)	Clay, quartz, calcite	<500 °C	
Room E				
5290	Wall BB1082	Clay, quartz, calcite	500 °C	Fig. 8
5291	Mud-brick	Clay, quartz, calcite	500 °C	Fig. 9
5292	Wall BB1082	Clay, quartz, calcite	500 °C	Fig. 8
5294	Mud-brick	Clay, quartz, calcite	500 °C	Fig. 9
5295	Mud-brick	Clay, quartz, calcite	500 °C	Fig. 9
5296	Mud-brick	Clay, quartz, calcite	500 °C	Fig. 9
5297	Mud-brick	Clay, quartz, calcite	500 °C	Fig. 9
5324	Mud-brick	Clay, quartz, calcite, aragonite	≥800 °C	Fig. 9
5641	Mud-brick	Clay, quartz, calcite	500 °C	Fig. 9
5642	Mud-brick	Clay, quartz, calcite	500 °C	Fig. 9
5643	Mud-brick	Clay, quartz, calcite	500 °C	Fig. 9
5644	Mud-brick	Clay, quartz, calcite	500 °C	Fig. 9
5646	Wall BB1082	Clay, quartz, calcite	500 °C	Fig. 8
5652	Wall BB1082	Clay, quartz, calcite	500 °C	Fig. 8
5653	Wall BB1082	Clay, quartz, calcite	500 °C	Fig. 8
5654	Wall BB1082	Clay, quartz, calcite	500 °C	Fig. 8
5655	Wall BB1082	Clay, quartz, calcite	500 °C	Fig. 8
5658	Mud-brick	Clay, quartz, calcite	500 °C	Fig. 9
5711	Floor (sediment)	Clay, quartz, calcite	<500 °C	
5712	Floor (sediment)	Clay, quartz, calcite (+charcoal)	<500 °C	
5713	Floor (sediment)	Clay, quartz, calcite	<500 °C	
5714	Floor (sediment)	Clay, quartz, calcite	<500 °C	
5727	Mud-brick	Clay, quartz, calcite	500 °C	Fig. 9
5740	Mud-brick	Clay, quartz, calcite,	600–700 °C	Fig. 8
5764	Mud-brick		≥800 °C	Fig. 8

(*continued on next page*)

Table 3 (*continued*)

Sample	Source	Minerology	Temperature	Figure
		Clay, quartz, calcite, aragonite		
5868	Floor (sediment)	Clay, quartz, calcite (+charcoal)	<500 °C	
5871	Wall BB1082	Clay, quartz, calcite	500 °C	Fig. 8
5872	Floor (sediment)	Clay, quartz, calcite	<500 °C	
5873	Wall BB1082	Clay, quartz, calcite	500 °C	Fig. 8
5874	Wall BB1082	Clay, quartz, calcite	500 °C	Fig. 8
5875	Wall BB1082	Clay, quartz, calcite	500 °C	Fig. 8
5876	Wall BB1082	Clay, quartz, calcite	500 °C	Fig. 8
5906	Mud-brick	Clay, quartz, calcite	500 °C	Fig. 8
5907	Mud-brick	Clay, quartz, calcite	600–700 °C	Fig. 8
5908	Sediment (wooden box)	Clay, quartz, calcite (+charcoal)	600–700 °C	Fig. 8
5909	Ash layer	Opal, aragonite calcite, hydroxylapatite	≥800 °C	Fig. 8
5910	Ash layer	Opal, aragonite calcite, hydroxylapatite	≥800 °C	Fig. 8
5911	Ash layer	Opal, aragonite calcite, hydroxylapatite	≥800 °C	Fig. 8
5912	Stone	Calcite, aragonite	600–700 °C	Fig. 9
5913	Mud-brick	Clay, quartz, calcite, aragonite	≥800 °C	Fig. 8
6336	Mud-brick	Clay, quartz, calcite	600–700 °C	Fig. 9
6337	Mud-brick	Clay, quartz, calcite	<500 °C	Fig. 9
6338	Sediment	Clay, quartz, calcite	<500 °C	Fig. 9
6465	Sediment	Clay, quartz, calcite	<500 °C	Fig. 9
6466	Mud-brick	Clay, quartz, calcite	500 °C	Fig. 9
6467	Mud-brick	Clay, quartz, calcite	<500 °C	Fig. 9
6468	Mud-brick	Clay, quartz, calcite	500 °C	Fig. 9
6469	Mud-brick	Clay, quartz, calcite	<500 °C	Fig. 9
6470	Mud-brick	Clay, quartz, calcite	<500 °C	Fig. 9
6471	Mud-brick	Clay, quartz, calcite	500 °C	Fig. 9
6472	Mud-brick	Clay, quartz, calcite	500 °C	Fig. 9
6473	Mud-brick	Clay, quartz, calcite	500 °C	Fig. 9
6474	Mud-brick	Clay, quartz, calcite, aragonite	800 °C	Fig. 8
6475	Stone	Calcite, aragonite	600–700 °C	Fig. 8
6476	Mud-brick	Clay, quartz, calcite	500 °C	Fig. 8
6477	Ash	Opal, aragonite calcite, hydroxylapatite	≥800 °C	Fig. 8
6478	Ash	Opal, aragonite calcite, hydroxylapatite	≥800 °C	Fig. 8
6488	Stone	Calcite, aragonite	600–700 °C	Fig. 8
6489	Ash	Opal, aragonite calcite, hydroxylapatite	≥800 °C	Fig. 8
6490	Mud-brick	Clay, quartz, calcite, aragonite	600–700 °C	Fig. 8
6491	Mud-brick	Clay, quartz, calcite, aragonite	≥800 °C	Fig. 8
Room D (North)				
2353	Mud-brick	Clay, quartz, calcite	<500 °C	Fig. 9
5293	Mud-brick	Clay, quartz, calcite	500 °C	Fig. 9
5305	Mud-brick	Clay, quartz, calcite	<500 °C	Fig. 9
5306	Mud-brick	Clay, quartz, calcite	500 °C	Fig. 9
5307	Mud-brick	Clay, quartz, calcite	500 °C	Fig. 9
5308	Mud-brick	Clay, quartz, calcite	<500 °C	Fig. 9
5311	Mud-brick	Clay, quartz, calcite	<500 °C	Fig. 9
5312	Sediment (debris)	Clay, quartz, calcite	<500 °C	Fig. 9
5313	Mud-brick	Clay, quartz, calcite	<500 °C	Fig. 9
5322	Floor (sediment)	Clay, quartz, calcite	<500 °C	
5384	Floor (sediment)	Clay, quartz, calcite (+charcoal)	<500 °C	
5428	Mud-brick	Clay, quartz, calcite	<500 °C	Fig. 8
5480	Floor (sediment)	Clay, quartz, calcite	<500 °C	
5481	Floor (sediment)	Clay, quartz, calcite	<500 °C	
5482	Floor (sediment)	Clay, quartz, calcite (+charcoal)	<500 °C	
5679	Mud-brick	Clay, quartz, calcite	500 °C	Fig. 8
5743	Sediment (debris)	Clay, quartz, calcite	<500 °C	Fig. 8

Table 3 (*continued*)

Sample	Source	Minerology	Temperature	Figure
5744	Sediment (debris)	Clay, quartz, calcite	<500 °C	Fig. 8
5745	Sediment (debris)	Clay, quartz, calcite (+charcoal)	500 °C	Fig. 8
5746	Sediment (debris)	Clay, quartz, calcite (+charcoal)	500 °C	Fig. 8
5747	Sediment (debris)	Clay, quartz, calcite (+charcoal)	500 °C	Fig. 8
5748	Sediment (debris)	Clay, quartz, calcite (+charcoal)	500 °C	Fig. 8
5749	Sediment (debris)	Clay, quartz, calcite (+charcoal)	500 °C	Fig. 8
5750	Sediment (debris)	Clay, quartz, calcite (+charcoal)	500 °C	Fig. 8
5758	Sediment (debris)	Clay, quartz, calcite (+charcoal)	500 °C	Fig. 8
5792	Sediment (debris)	Clay, quartz, calcite	<500 °C	Fig. 9
5793	Sediment (debris)	Clay, quartz, calcite	500 °C	Fig. 9
5794	Sediment (debris)	Clay, quartz, calcite	500 °C	Fig. 9
5795	Mud-brick	Clay, quartz, calcite	500 °C	Fig. 9
5796	Sediment (debris)	Clay, quartz, calcite	500 °C	Fig. 9
5797	Mud-brick	Clay, quartz, calcite	<500 °C	Fig. 9
5798	Sediment (debris)	Clay, quartz, calcite	500 °C	Fig. 9
5799	Sediment (debris)	Clay, quartz, calcite	<500 °C	Fig. 9
5800	Floor (sediment)	Clay, quartz, calcite	<500 °C	
5877	Mud-brick	Clay, quartz, calcite	<500 °C	Fig. 9
5878	Sediment (debris)	Clay, quartz, calcite	<500 °C	Fig. 9
5879	Mud-brick	Clay, quartz, calcite	500 °C	Fig. 9
5880	Sediment (debris)	Clay, quartz, calcite	<500 °C	Fig. 9
5934	Mud-brick	Clay, quartz, calcite, aragonite	≥800 °C	Fig. 9
5935	Mud-brick	Clay, quartz, calcite, aragonite	600–700 °C	Fig. 9
5936	Sediment (debris)	Clay, quartz, calcite	<500 °C	Fig. 9
5971	Floor (sediment)	Clay, quartz, calcite	<500 °C	
5974	Mud-brick	Clay, quartz, calcite	<500 °C	Fig. 8
6005	Mud-brick	Clay, quartz, calcite, aragonite	500 °C	Fig. 8
6011	Floor (sediment)	Clay, quartz, calcite	<500 °C	
6055	Floor (sediment)	Clay, quartz, calcite (+charcoal)	<500 °C	
6230	Floor (sediment)	Clay, quartz, calcite (+charcoal)	<500 °C	
6463	Floor (sediment)	Clay, quartz, calcite	<500 °C	
6479	Floor (sediment)	Clay, quartz, calcite	<500 °C	
6492	Floor (sediment)	Clay, quartz, calcite	<500 °C	
Room D (South)				
5548	Sediment (debris)	Clay, quartz, calcite	500 °C	Fig. 9
5549	Sediment (debris)	Clay, quartz, calcite	500 °C	Fig. 9
5550	Mud-brick	Clay, quartz, calcite	500 °C	Fig. 9
5551	Mud-brick	Clay, quartz, calcite	500 °C	Fig. 9
5552	Mud-brick	Clay, quartz, calcite	500 °C	Fig. 9
5625	Sediment inside jar	Clay, quartz, calcite	<500 °C	Fig. 9
5638	Floor (sediment)	Clay, quartz, calcite	<500 °C	
5755	Mud-brick	Clay, quartz, calcite	<500 °C	Fig. 8
5756	Mud-brick	Clay, quartz, calcite, aragonite	≥800 °C	Fig. 8

(*continued on next page*)

Table 3 (*continued*)

Sample	Source	Minerology	Temperature	Figure
5757	Mud-brick	Clay, quartz, calcite, aragonite	≥800 °C	Fig. 8
6318	Floor (stone)	Calcite	<500 °C	
6319	Sediment (debris)	Clay, quartz, calcite	500 °C	Fig. 9
6320	Mud-brick	Clay, quartz, calcite	500 °C	Fig. 9
6321	Mud-brick	Clay, quartz, calcite	500 °C	Fig. 8
6322	Sediment (debris)	Clay, quartz, calcite	<500 °C	Fig. 8
6323	Sediment (debris)	Clay, quartz, calcite	<500 °C	Fig. 8
6324	Mud-brick	Clay, quartz, calcite	500 °C	Fig. 8
6325	Mud-brick	Clay, quartz, calcite	<500 °C	Fig. 9
6326	Mud-brick	Clay, quartz, calcite	600–700 °C	Fig. 8
6327	Floor (stone)	calcite	<500 °C	
6329	Mud-brick	Clay, quartz, calcite	<500 °C	Fig. 9
6330	Mud-brick	Clay, quartz, calcite	500 °C	Fig. 8
6331	Floor (stone)	calcite	<500 °C	
6332	Sediment (debris)	Clay, quartz, calcite	<500 °C	Fig. 9
6333	Sediment (debris)	Clay, quartz, calcite	500 °C	Fig. 9
6334	Mud-brick	Clay, quartz, calcite	500 °C	Fig. 8
6504	Mud-brick	Clay, quartz, calcite	<500 °C	Fig. 9
6505	Mud-brick	Clay, quartz, calcite	<500 °C	Fig. 9
6506	Mud-brick	Clay, quartz, calcite	<500 °C	Fig. 9
6507	Mud-brick	Clay, quartz, calcite	<500 °C	Fig. 9
6508	Mud-brick	Clay, quartz, calcite	600–700 °C	Fig. 8
6509	Mud-brick	Clay, quartz, calcite	600–700 °C	Fig. 9
6510	Sediment (debris)	Clay, quartz, calcite	500 °C	Fig. 8
6511	Mud-brick	Clay, quartz, calcite	600–700 °C	Fig. 9
6512	Mud-brick	Clay, quartz, calcite	500 °C	Fig. 9
6513	Mud-brick	Clay, quartz, calcite	500 °C	Fig. 8
6586	Floor (sediment)	Clay, quartz, calcite	<500 °C	
6587	Floor (sediment)	Clay, quartz, calcite	<500 °C	

as excessive quantities of combustible materials to suggest that fuel was intentionally added to facilitate the fire. As mentioned in Section 1.1, fire investigators also use indirect considerations when deciding if a fire resulted from an accident or was intentionally set (Lentini, 2013: 138–139; NFPA 921: 921.221, 256–257). We therefore turn to site-wide evidence and look at the broader story of the destruction of Level VI at Lachish by examining the processes experienced by the city prior to and after the destruction. Remains of Level VI that are relevant to this case study are the Acropolis Temple (Area P) and the Pillared Structure (Area S; Fig. 3).

The Acropolis Temple, located at the highest point at the site and probably the main temple of the city, shows no evidence of crisis architecture. Ussishkin (2004b: 251–253) suggested that it was abandoned or looted, as all rooms except for Storeroom 3162 were found almost empty of pottery or other finds (Clamer, 2004; Ussishkin, 2004b: 231, 253, 258, figs. 6.2, 6.11. 6.48). After the apparent abandonment or looting, the Acropolis Temple burned down, as deduced from remains of charred cedar beams found lying on the floor (Ussishkin, 2004b: 224, 227, 238, 247).

The Pillared Building, measuring ca. 18 × 3.5 m, originally served a public purpose (Barkay and Ussishkin, 2004: 353–355). Its final stage yielded evidence for domestic activity in the form of pottery (i.e., storage jars, bowls and kraters), ovens and other installations (Barkay and Ussishkin, 2004: 357–358). Skeletons of women, children and infants were found facing down, possibly trapped by the structure's collapse (Barkay and Ussishkin, 2004: 361, 363, 401; Smith, 2004). Evidence for fire includes charred wood and burnt bricks (Barkay and Ussishkin, 2004: 353–362, 365).

Table 4 summarizes the evidence of the destruction of Level VI, showing that it was not uniform across the site. Both the NET and the Pillared Building were originally public structures, although in their last phases they display evidence of domestic activities. Furthermore, domestic activity in the NET took place along with continued cultic activity, suggesting social crisis. Crisis architecture also occurs in the Pillared Building, while the Acropolis Temple was abandoned (and not re-used) some time, at least several days but possibly much longer, before the destruction.

In terms of the timing of the destruction, we maintain that it occurred at about the same time across the site (possibly after a period of siege or societal decline), because the latest pottery in all excavated areas (a total of hundreds of square metres), and the existing radiometric ages are contemporary (12 samples, 1203–1130 BCE, 68.2 % range, 1210–1126, 95.5 % range; Garfinkel et al., 2019a; Weissbein et al., 2019). While pottery typology and radiocarbon ages show a range of some 50–100 years, field evidence supports a scenario of one large destruction event rather than several small diachronic events. (1) In all excavated areas of all expeditions there is only one level of destruction by fire. (2) Nowhere across the excavated areas of all expeditions have unburned structures of Level VI been uncovered on top of burnt structures of the same level; rather, an occupation gap of at least 150 years after the destruction of Level VI until the construction of Level V, apart from some pits, is found in all excavated areas. (3) Hoards of precious objects were found in several places across Level VI (Weissbein et al., 2019; Ussishkin, 2004c: 626), while skeletons of women and children were uncovered in Area S (Smith, 2004). All these lines of evidence indicate that occupation of the city known as Level VI ceased at once (*sensu lato*). Had this not been the case, old and new buildings would have existed together and local (rather than site-wide) destruction would have resulted in treatment of the dead victims, reclamation of valuables, and renovation. Moreover, in the case of a considerable gap between the destruction events, pottery assemblages and radiocarbon ages would not be synchronous across Level VI. Consequently, the fire that devastated the NET and other sectors of the city is related to a destruction event that lasted no more than a few weeks.

Evidence of fire was found across Level VI in all areas opened up by excavation over the years (Tufnell, 1958: 49–50; Aharoni, 1975: 12; Ussishkin, 2004c: 624–631; Garfinkel et al., 2019a; 2019b). A scenario of accidental fire that spread across the entire city is unlikely, especially in light of studies showing that roofs covered with mud plaster (as clearly seen in the NET) are difficult to ignite from the outside (Gordon, 1953; Kreimerman and Shahack-Gross, 2019). Consequently, a fire that starts in one building is unlikely to spread to another, let alone burn down the entire city. Thus, as the city shows widespread evidence of fire, it is most likely – although not certain – that different structures burned down separately, a situation that is suggestive of arson (*contra* Cline, 2014: 121; Millek, 2017: 128–131).

6. Discussion

The case study of the destruction of the NET and the end of Canaanite Lachish demonstrates the value of using an integrated approach for reconstructing ancient conflagration events.

The greatest advantage of this approach is in its simplicity. The locations of ash, soot, charred matter and mud brick collapse were documented using standard archaeological methods, and temperatures were mapped across the structure using FTIR spectroscopy — a commonly used technique, especially in the Southern Levant (see Table 1; Sections 1.1 and 1.2). The adaptation of insights from modern fire investigation to the archaeological case study (Fig. 1; Section 1.5) gave new meaning to those data and facilitated the identification of the locations where fire reached a fully-developed stage and potential ignition areas, and enabled estimation of the relative duration of fire in different architectural units. This in turn allowed reconstructing the fire propagation path.

Furthermore, in previous studies in which concepts from modern fire investigation were applied to the archaeological case (e.g., Cunningham,

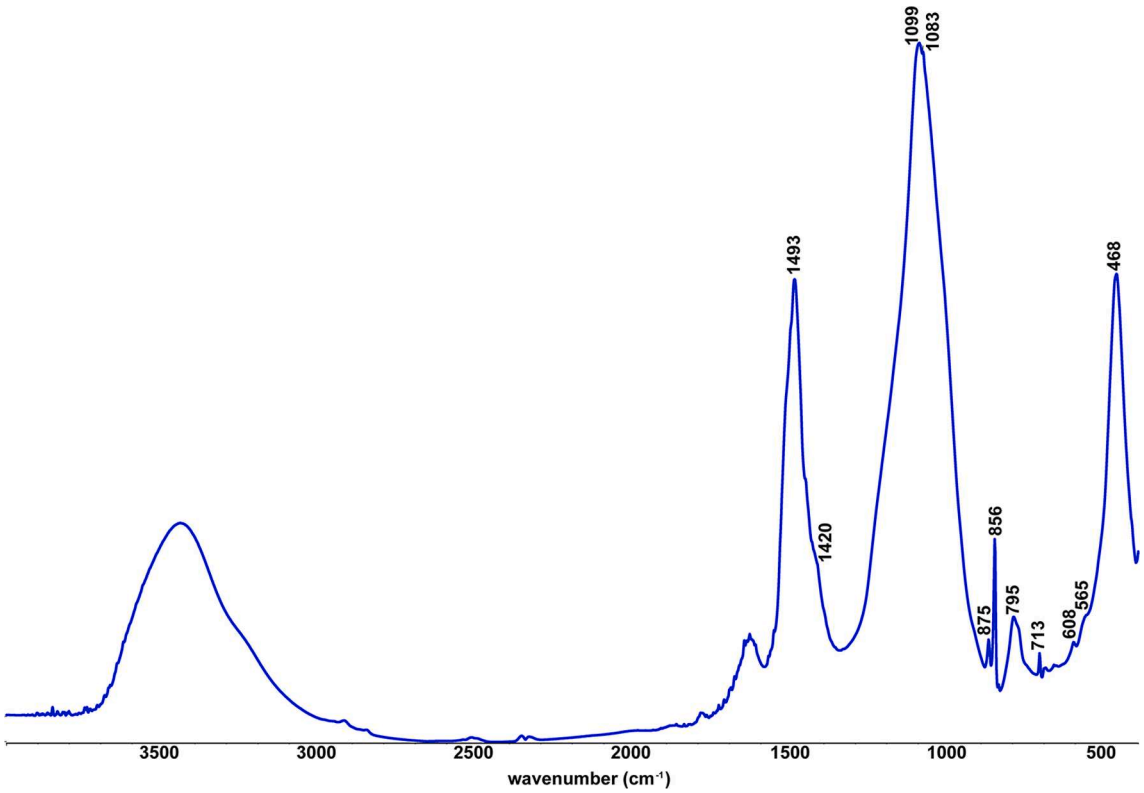

Fig. 12. FTIR spectrum of a sample from the grey layer. Note the presence of opal (bands at 1099, 795 and 468 cm^{-1}), aragonite (bands at 1493, 1083, 856 and 713 cm^{-1}), calcite (a shoulder at 1420 cm^{-1} with additional bands at 875 and 713 cm^{-1}) and hydroxylapatite (bands at 608 and 565 cm^{-1}). The presence of aragonite suggests a high burning temperature (above 650 °C).

Table 4
Comparison of destruction evidence from three completely excavated Level VI structures. Years of excavation are noted in parentheses.

	North-East Temple (2014–2016)	Acropolis Temple (1973–1977)	Pillared Structure (1978–1983)
Crisis architecture	+	—	+
Fire	+	+	+
Abandonment/ looting mode	Rapid	Organized	Rapid
Skeletons	—	—	+
Post destruction	Occupation gap (+pits)	Occupation gap (+pits)	Occupation gap (+pits)

2007; Twiss et al., 2008; Table 1), this was due to exceptional field observations, such as specific soot marks on well-preserved plastered walls or molten pottery across an entire structure (Section 1.3). The model presented here does not depend on such exceptional observations and allows the reconstruction of fire from more commonly found evidence, and therefore has a higher potential to be utilized in many other sites.

The reconstruction of the fire in the NET could not determine with certainty whether it resulted from arson or accident. Yet, due to the understanding of fire dynamics in mud-brick structures and the specific architecture of such structures in the region (i.e. mud-covered roofs), it was possible to integrate data collected by previous excavations that used traditional techniques to argue that the fire of Level VI most probably resulted from arson. It should be stressed, however, that such data should be considered with care and only when the construction materials and techniques are known. This conclusion was also supported by indirect evidence (i.e., evidence of crisis, prolonged abandonment after the destruction) highlighting the importance of traditional methods that treat destruction as a process (Section 1.1).

7. Conclusions

This study has presented an integrative framework (Fig. 1) for interpreting archaeological destruction by fire. The framework is based on three pillars:

(1) Field archaeology: the locations of ash, charred material and soot across space and along stratigraphic sequences
(2) Micro-geoarchaeology: vertical and horizontal distribution of temperatures using FTIR spectroscopy
(3) Fire investigation: identifying areas of ignition and fire propagation paths based on both field archaeology and micro-geoarchaeology

This approach can be applied to reconstructing and understanding conflagration events in other sites, periods and areas where mud-brick structures and mud-plastered roofs have served as construction materials. Doing so in other places will require preparatory stages of micro-geoarchaeological investigation in which local construction materials and techniques are explored as presented here, since these have important implications for fire behaviour in compartments. Post-destruction processes such as reclamation of objects, erosion, later construction or bioturbation could affect the material and mineralogical evidence. This study has considered a conflagration event in a single-storey building. While in general the same model could be used for understanding fires in multi-storey structures, the practical challenges are much greater, as a clear distinction between destruction debris of each floor could be challenging. Furthermore, walls are rarely preserved *in situ* beyond the ground-floor level. Consequently, the architectural layout of upper floors, crucial for understanding fire behaviour, becomes

difficult to reconstruct and complicates the situation further. Thus, analyses of conflagration events of multi-storey structures deserve further study and possibly the development of an adapted model.

CRediT authorship contribution statement

Igor Kreimerman: Conceptualization, Methodology, Investigation, Writing – original draft, Writing – review & editing, Visualization. **Yosef Garfinkel:** Writing – review & editing, Supervision, Funding acquisition. **Michael G. Hasel:** Writing – review & editing, Supervision, Funding acquisition. **Ruth Shahack-Gross:** Conceptualization, Methodology, Writing – review & editing, Supervision, Funding acquisition.

Declaration of Competing Interest

The authors declare that they have no known competing financial interests or personal relationships that could have appeared to influence the work reported in this paper.

Data availability

Data will be made available on request.

Acknowledgements

Laboratory analyses were supported by funds available to R.S.-G. at the Laboratory for Sedimentary Archaeology, University of Haifa. I.K. was supported by fellowships from the Mandel School for Advanced Studies in the Humanities and the Institute of Archaeology of the Hebrew University of Jerusalem. Our gratitude is extended to I. Weissbein, who works on the analysis of the finds from the North-East Temple, for sharing his insights with us. Last but not least are the dozens of volunteers who participated in the excavations of the Fourth Expedition to Lachish.

References

Adler, W., 2001. Palast P4. In: Adler, W., Penner, S. (Eds.), Kāmid El-Lōz 18: Die Spätbronzezeitlichen Palastanlagen. Rudolph Habelt Gmbh, Bonn, pp. 37–216.
Aharoni, Y., 1975. Investigations at Lachish: The Sanctuary and the Residency (Lachish V). Institute of Archaeology, Tel Aviv University, Tel Aviv.
Albright, W.F., 1935. Archaeology and the Date of the Hebrew Conquest of Palestine. Bull. Am. Sch. Orient. Res. 58, 10–18.
Aldeias, V., Dibble, H.L., Sandgathe, D., Goldberg, P., McPherron, S.J.P., 2016. How Heat Alters Underlying Deposits and Implications for Archaeological Fire Features: A Controlled Experiment. J. Archaeol. Sci. 67, 64–79.
Alperson-Afil, N., 2012. Archaeology of Fire: Methodological Aspects of Reconstructing Fire History of Prehistoric Archaeological Sites. Earth-Sci. Rev. 113 (3–4), 111–119.
Amadio, M., Boaretto, E., Bombardieri, L., 2020. Abandonment Practices through the Microscope Lens. Microarchaeol. Data from Middle Bronze Age Erimi, Cyprus, Levant 52, 301–320.
Arav, R., 2014. A Chronicle of Inevitable Destruction: Stages in the Conquest and Destruction of Bethsaida by Tiglath Pileser III. In: Ellens, H.J. (Ed.), BeThsAidA in ArchAeology, HisTory And AncienT CulTure: A FesTschrifT in Honor of John T. Cambridge Scholars Publishing, Newcastle upon Tyne, Greene, pp. 2–25.
Bankoff, H.A., 1979. A house-burning in Serbia: what do burned remains tell an archaeologist? Archaeology 32, 8–14.
Barkay, G., Ussishkin, D., 2004. Area S: The Late Bronze Age strata. In: Ussishkin, D. (Ed.), The Renewed Archaeological Excavations at Lachish (1973–1994). Institute of Archaeology, Tel Aviv University, Tel Aviv, pp. 316–407.
Berna, F., Behar, A., Shahack-Gross, R., Berg, J., Boaretto, E., Gilboa, A., Sharon, I., Shalev, S., Shilstein, S., Yahalom-Mack, N., Zorn, J.R., Weiner, S., 2007. Sediments Exposed to High Temperatures: Reconstructing Pyrotechnological Processes in Late Bronze and Iron Age Strata at Tel Dor (Israel). J. Archaeol. Sci. 34, 358–373.
Berna, F., Goldberg, P., Kolska Horwitz, L., Brink, J., Holt, S., Bamford, M., Chazan, M., 2012. Microstratigraphic Evidence of in situ Fire in the Acheulean Strata of Wonderwerk Cave, Northern Cape Province, South Africa. Proc. Natl. Acad. Sci. Plus 109, E1215–E1220.
Bjorkman, J., 1999. How to Bury a Temple: The Case of Nuzi's Ishtar Temple A. In: Owen, D.I., Wilhelm, G. (Eds.), Studies on the Civilization and Culture of Nuzi and Hurrians 9. CDL Press, Bethesda, MD, pp. 103–122.
Braadbaart, F., Poole, I., 2008. Morphological, Chemical and Physical Changes during Charcoalification of Wood and Its Relevance to Archaeological Contexts. J. Archaeol. Sci. 35, 2434–2445.
Chandler, R.K., 2009. Fire Investigation. Delmar, Cengage Learning, Clifton Park, NY.
Christensen, A.M., Icove, J.D., 2004. The Application of NIST's Fire Dynamics Simulator to the Investigation of Carbon Monoxide Exposure in the Deaths of Three Pittsburgh Fire Fighters. J. of Forensic Sci. 49 (1), 104–107.
Christensen, L.B., Jense, S.E. Johansen, A.L.L., Johansen, P.R., Lerager, S. 2007. House 1 – Experimental Fire and Archaeological Excavation. In: Rasmussen, M. (Ed.), Iron Age House in Flames. Testing House Reconstructions at Lejre, Lejre, Historical-Archaeological Experimental Center, pp. 42–133.
Clamer, C., 2004. The Pottery and Artifacts from the Level VI Temple in Area P. In: Ussishkin, D. (Ed.), The Renewed Archaeological Excavations at Lachish (1973–1994). Institute of Archaeology, Tel Aviv University, Tel Aviv, pp. 1288–1325.
Cline, E.H., 2014. 1177 B.C.: The Year Civilization Collapsed. Princeton University Press, Princeton, NJ.
Cunningham, T.F., 2007. Havoc: the destruction of power and the power of destruction in Minoan Crete. In: Bretschneider, J., Driessen, J., Van Lerberghe, K. (Eds.), Power and Architecture: Monumental Public Architecture in the Bronze Age Near East and Aegean. Peeters, Leuven, pp. 23–43.
De Haan, J.D., Icove, D.J., 2014. Kirk's Fire Investigation. Pearson, Harlow.
DiNenno, P.J., Drysdale, D., Beyler, C.L., Walton, W.D., Custer, R.L.P., Hall, J.R.J., Watts, J.M.J. (Eds.), 2002. SFPE Handbook of Fire Protection Engineering. National Fire Protection Association, Bethesda, MD.
Driessen, J., 1995. 'Crisis Architecture': Some Observations on Architectural Adaptations as Immediate Responses to Changing Socio-cultural Conditions. Topoi 5, 63–88.
Driessen, J., 1999. The Archaeology of Aegean Warfare. In: Laffineur, R. (Ed.), PoLemos: Le Contexte Guerrier En Egée À L'âge Du Bronze. Université de Liège, Liège, pp. 11–19.
Driessen, J. (Ed.), 2013. Destruction: Archaeological, Philological and Historical Perspectives. Presses Universitaires de Louvain, Louvain-la-Neuve.
Driessen, J., Macdonald, C.F., 1997. The Troubled Island: Minoan Crete Before and After the Santorini Eruption. Université de Liège, Liège.
Driessen, J., 2013a. Time Capsules? Destructions as Archaeological Phenomena. In: Driessen, J. (Ed.), Destruction. Archaeological, Philological and Historical Perspectives. Presses Universitaires de Louvain, Louvain-la-Neuve, pp. 5–22.
Dunseth, Z.C., Fuks, D., Langgut, D., Weiss, E., Melamed, Y., Butler, D.H., Yan, X., Boaretto, E., Tepper, Y., Bar-Oz, G., Shahack-Gross, R., 2019. Archaeobotanical Proxies and Archaeological Interpretation: A Comparative Study of Phytoliths, Pollen and Seeds in Dung Pellets and Refuse Deposits at Early Islamic Shivta, Negev, Israel. Quat. Sci. Rev. 211, 166–185.
Faust, A., Katz, H., Sapir, Y., Avraham, A., Marder, O., Bar-Oz, G., Weiss, E., Auman-Chazan, C., Hartmann-Shenkman, A., Sadiel, T., Vilany, O., Tsesarsky, M., Sarah, P., Ackermann, O., Timmer, N., Katz, O., Langgut, D., Benzaquen, M., 2017. The Birth, Life and Death of an Iron Age House at Tel 'Eton, Israel. Levant 49, 136–173.
Finkelstein, I., 2009. Destructions: Megiddo as a Case Study. In: Schloen, D. (Ed.), Exploring thE LonguE DuréE: Essays in Honor of LawrEncE E. Stager, Eisenbrauns, Winona Lake, IN, pp. 113–126.
Forget, M.C.L., Regev, L., Friesem, D.E., Shahack-Gross, R., 2015. Physical and Mineralogical Properties of Experimentally Heated Chaff-Tempered Mud Bricks: Implications for Reconstruction of Environmental Factors Influencing the Appearance of Mud Bricks in Archaeological Conflagration Events. J. Archaeol. Sci. Rep. 2, 80–93.
Forget, M.C.L., Shahack-Gross, R., 2016. How Long Does it Take to Burn Down an Ancient Near Eastern City? The Study of Experimentally Heated Mud-Bricks. Antiq. 90, 1213–1225.
Friede, H.M., Steel, R.H., 1980. Experimental burning of traditional Nguni huts. African Studies 39, 171–181.
Garfinkel, Y., 2020. The Sceptres of Life-sized Divine Statues from Canaanite Lachish and Hazor. Antiq. 94, 669–685.
Garfinkel, Y., Hasel, M.G., Klingbeil, M.G., Kang, H.-G., Choi, G., Chang, S.-Y., Hong, S., Ganor, S., Kreimerman, I., Bronk Ramsey, C., 2019a. Lachish Fortifications and State Formation in the Biblical Kingdom of Judah in Light of Radiometric Datings. Radiocarb. 61, 695–712.
Garfinkel, Y., Kreimerman, I., Hasel, M.G., Klingbeil, M.G., 2019b. First Impression on the Urban Layout of the Last Canaanite City of Lachish: A View from the Northeast Corner of the Site. In: Maeir, A.M., Shai, I., McKinny, C. (Eds.), The Late Bronze and Early Iron Ages of SouThern Canaan. De Gruyter, Berlin, pp. 122–135.
Garfinkel, Y., Hasel, M.G., Klingbeil, M.G., Kreimerman, I., Pytlik, M., Carroll, J.W., Waybright, J.W.B., Kang, H.-G., Choi, G., Chang, S.-Y., Hong, S., David, A., Weissbein, I., Silberberg, N., 2021. The Canaanite and Judean Cities of Lachish, Israel: Preliminary Report of the Fourth Expedition, 2013–2017. Am. J. of Archaeol. 125 (3), 419–459.
Gheorghiu, D. 2016. Building and Burning: The Construction and Combustion of Chalcolithic Dwellings in the Lower Danube and the Eastern Carpathian Areas from the Perspective of Experimental Archaeology. In: Nikolova, L., Merlini, Cosma, A. (eds.), Western-Pontic Culture Ambience and Pattern. De Gruyter, Berlin, pp. 33–52.
Godleman, J., Almond, M.J., Matthews, W., 2016. An Infrared Microspectroscopic Study of Plasters and Pigments from the Neolithic Site of Bestansur, Iraq. J. Archaeol. Sci. Rep. 7, 195–204.
Gordon, D.H., 1953. Fire and the Sword: The Technique of Destruction. Antiq. 27, 149–152.
Harrison, K., 2013. The Application of Forensic Fire Investigation Techniques in the Archaeological Record. J. Archaeol. Sci. 40, 955–959.
Harrison, K., 2008. Fire and Burning at Çatalhöyük. Çatalhöyük Archive Reports, 273–280. http://www.catalhoyuk.com/sites/default/files/media/pdf/Archive_Report_2008.pdf [Accessed 10.03.2019].
Hasel, M.G., 2016. The Archaeology of Destruction: Methodological Desiderata, in: Ganor, S., Kreimerman, I., Streit, K., Mumcuoglu, M. (Eds.), From Sha'ar Hagolan to

Shaaraim: Essays in Honor of Prof. Yosef Garfinkel. Israel Exploration Society, Jerusalem, pp. 205–228.
Heskestad, G., 2002. Fire Plumes, Flame Height, and Air Entrainment, in: DiNenno, P.J., Drysdale, D., Beyler, C.L., Walton, W.D., Custer, R.L.P., Hall, J.R.J., Watts, J.M.J. (Eds.), SFPE Handbook of Fire Protection Engineering. National Fire Protection Association, Quincy, MA, pp. 2.1–2.17.
Hlubik, S., Berna, F., Feibel, C., Braun, D., Harris, J.W.K., 2017. Researching the Nature of Fire at 1.5 Mya on the Site of FxJj20 AB, Koobi Fora, Kenya, Using High-Resolution Spatial Analysis and FTIR Spectrometry. Curr. Anthropol. 58, S243–S257.
Icove, D.J., Welborn, H.E., Vonarx, A.J., Adams, E.C., Lally, J.R., Huff, T.G., 2006. Scientific Investigation and Modeling of Prehistoric Structural Fires at Chevelon Pueblo. In: Proceedings of the 2006 International Symposium on Fire Investigation Science and Technology. National Association of Arson Investigators, Sarasota, FL, pp. 457–467.
Icove, D.J., Lally, J.R., Miller, L.K., Harris, E.C., 2014. The Use of the "Harris Matrix" in Fire Scene Documentation. In: Proceedings of the 7th International Symposium on Fire Investigation Science and Technology, Sarasota, FL, pp. 317–323.
Icove, D.J., DeHaan, J.D., Haynes, G.A., Forensic Fire Scene Reconstruction. 3rd ed. Pearson, Boston.
Kerber, S., 2012. Analysis of Changing Residential Fire Dynamics and Its Implications on Firefighter Operational Timeframes. Fire Technol. 49, 857–889.
Kreimerman, I., 2016. Siege Warfare, Conflict and Destruction: How are They Related? In: Ganor, S., Kreimerman, I., Streit, K., Mumcuoglu, M. (Eds.), From Sha'ar Hagolan to Shaaraim: Essays in Honor of Prof. Yosef Garfinkel. Israel Exploration Society, Jerusalem, pp. 229–245.
Kreimerman, I., 2017a. A Typology for Destruction Layers: The Late Bronze Age Southern Levant as a Case Study. In: Driessen, J., Cunningham, T.F. (Eds.), Crisis to Collapse: The Archaeology of Social Breakdown. Presses Universitaires de Louvain, Louvain-la-Neuve, pp. 173–203.
Kreimerman, I., 2017b. Skeletons in Bronze and Iron Age Destruction Contexts in the Southern Levant: What Do They Mean? West & East 2, 13–30.
Kreimerman, I., Shahack-Gross, R., 2019. Understanding Conflagration of One-story Mud-brick Structures: An Experimental Approach. Archaeol. Anthropol. Sci. 11, 2911–2928.
Kreimerman, I. 2022. Sennacherib, Nebuchadnezzar II, and the Residents of Lachish: An Examination of Decision-Making from Conquest to Destruction. In: Berlejung, A., Maeir, A.M., Oshima, T.M. (eds.), Writing and Re-Writing History through Destruction: Proceedings of the Third Annual RIAB Center Conference, Leipzig, May 2018. Mohr Siebeck, Tübingen, pp. 39–60.
Lally, J.R., Vonarx, A.J., 2011. Fire: Accidental or Intentional? An Archaeological Toolkit for Evaluating Accident and Intent in Ancient Structural Fires. In: Walker, W.H., Venzor, K.R. (Eds.), Contemporary Archaeologies of the Southwest. University Press of Colorado, Boulder, CO, pp. 157–171.
LaMotta, V.M., Schiffer, M.B., 1999. Formation Process of House Floor Assemblages. In: Allison, P.M. (Ed.), The Archaeology of Household Activities. Routledge, London, pp. 149–175.
Lazar, M., Cline, E.H., Nickelsberg, R., Shahack-Gross, R., Yasur-Landau, A., 2020. Earthquake damage as a catalyst to abandonment of a Middle Bronze Age settlement: Tel Kabri, Israel. PLoS ONE 15 (9), e0239079.
Lentini, J.J., 2013. Scientific Protocols for Fire Investigation. CRC Press, Boca Raton, FL.
Marco, S., 2008. Recognition of Earthquake-Related Damage in Archaeological Sites: Examples from the Dead Sea Fault Zone. Tectonophys. 453, 148–156.
Matthiae, P., 2009. Crisis and Collapse: Similarity and Diversity in the Three Destructions of Ebla from EB IVA to MB II. Scienze dell'Antichità. Storia Archeologia Antropologia 15, 43–83.
Mazar, A., 1980. Excavations at Tell Qasile, Part One: The Philistine Sanctuary: Architecture and Cult Objects. Institute of Archaeology, Hebrew University, Jerusalem.
Mazar, A., 1992. Temples from the Middle and Late Bronze Ages and the Iron Age. In: Kempinski, A., Reich, R. (Eds.), The Architecture of Ancient Israel: From the Prehistoric to the Persian Periods. Israel Exploration Society, Jerusalem, pp. 161–187.
Millek, J.M., 2017. Sea Peoples, Philistines, and the Destruction of Cities: A Critical Examination of Destruction Layers 'Caused' by the 'Sea Peoples'. In: Fischer, P.M., Bürge, T. (Eds.), 'Sea Peoples' Up-to-Date: New Research on Transformations in the Eastern Mediterranean in the 13th–11th Centuries BCE. Österreichische Akademie der Wissenschaften, Vienna, pp. 113–140.
Namdar, D., Zukerman, A., Maeir, A.M., Katz, J.C., Cabanes, D., Trueman, C., Shahack-Gross, R., Weiner, S., 2011. The 9th Century BCE Destruction Layer at Tell es-Safi/Gath, Israel: Integrating Macro- and Micro-archaeology. J. Archaeol. Sci. 38, 3471–3482.
Nelson, M.C., Schachner, G., 2002. Understanding Abandonment in the North American Southwest. J. Archaeol. Res. 19, 167–206.
NFPA 921 *Guide for Fire and Explosion Investigations* (2017 edition), Technical Committee on Fire Investigation of the National Fire Protection Association. https://www.nfpa.org/codes-and-standards/all-codes-and-standards/list-of-codes-and-standards/detail?code=921 (Accessed 23.11.2019).
Ohlemiller, T.J., 2002. Smoldering Combustion, in: DiNenno, P.J., Drysdale, D., Beyler, C.L., Walton, W.D., Custer, R.L.P., Hall, J.R.J., Watts, J.M.J. (Eds.), SFPE Handbook of Fire Protection Engineering. National Fire Protection Association, Quincy, MA, pp. 2.200–2.210.
Passerini, A., Regev, L., Rova, E., Boaretto, E., 2016. New Radiocarbon Dates for the Kura-Araxes Occupation at Aradetis Orgora. Georgia. Radiocarb. 58, 649–677.
Puytison-Lagarce, É., Lagarce, J., 2006. L'incendie du Palais Nord de Ras Ibn Hani. Traces et modalités d'une catastrophe. Syria 83: 247–258.
Quintiere, J.G., 1998. Principles of Fire Behavior. Delmar, Cengage Learning, Clifton Park, NY.
Quintiere, J.G., 2006. Fundamentals of Fire Phenomena. John Wiley & Sons, Chichester.
Regev, L., Poduska, K.M., Addadi, L., Weiner, S., Boaretto, E., 2010. Distinguishing Between Calcites Formed by Different Mechanisms using Infrared Spectrometry: Archaeological Applications. J. Archaeol. Sci. 37, 3022–3029.
Regev, L., Cabanes, D., Homsher, R., Kleiman, A., Weiner, S., Finkelstein, I., Shahack-Gross, R., 2015. Geoarchaeological Investigation in a Domestic Iron Age Quarter, Tel Megiddo. Israel. Bull. Am. Sch. Orient. Res. 374, 135–157.
Reich, R., 1992. Building Materials and Architectural Elements in Ancient Israel. In: Kempinski, A., Reich, R. (Eds.), The Architecture of Ancient Israel: from the Prehistoric to the Persian Periods. Israel Exploration Society, Jerusalem, pp. 1–16.
Rockett, J.A., Milke, J.A., 2002. Conduction of Heat in Solids, in: DiNenno, P.J., Drysdale, D., Beyler, C.L., Walton, W.D., Custer, R.L.P., Hall, J.R.J., Watts, J.M.J. (Eds.), SFPE Handbook of Fire Protection Engineering. National Fire Protection Association, Quincy, MA, pp. 1.27–1.43.
Rodríguez-Cintas, Á., Cabanes, D., 2017. Phytolith and FTIR Studies Applied to Combustion Structures: The Case of the Middle Paleolithic Site of El Salt (Alcoy, Alicante). Quat. Int. 431, 16–26.
Rodríguez-Pascua, M.A., Pérez-López., R., Giner-Robles, J.L., Silva, P.G., Garduño-Monroy, V.H., Reicherter, K., 2011. A Comprehensive Classification of Earthquake Archaeological Effects (EAE) in Archaeoseismology: Application to Ancient Remains of Roman and Mesoamerican Cultures. Quaternary International 242: 20–30.
Sanz, M., Daura, J., Egüez, N., Cabanes, D., 2017. On the Track of Anthropogenic Activity in Carnivore Dens: Altered Combustion Structures in Cova del Gegant (NE Iberian Peninsula). Quat. Int. 437, 102–114.
Sapir, Y., Avraham, A., Faust, A., 2018. Mud-brick Composition, Archeological Phasing and Pre-planning in Iron Age Structures: Tel 'Eton (Israel) as a Test-case. Archaeol. Anthropol. Sci. 10, 337–350.
Schiffer, M.B., 1987. Formation Processes of the Archaeological Record. University of New Mexico Press, Albuquerque, NM.
Seeher, J., 2001. Die Zerstörung der Stadt Ḫattuša. In: Wilhelm, G. (Ed.), Akten des IV. Internationalen Kogress für Hethitologie, Harrassowitz, Wiesbaden, pp. 623–634.
Shahack-Gross, R., Albert, R.M., Gilboa, A., Nagar-Hilman, O., Sharon, I., Weiner, S., 2005. Geoarchaeology in an Urban Context: The Uses of Space in a Phoenician Monumental Building at Tel Dor (Israel). J. Archaeol. Sci. 32, 1417–1431.
Shahack-Gross, R., Shaar, R., Hassul, E., Ebert, Y., Forget, M.C.L., Nowacyk, N., Marco, S., Finkelstein, I., 2018. Fire and Collapse: Untangling the Formation of Destruction Layers using Archaeomagnetism. Geoarchaeology 33, 513–528.
Shoval, S., Beck, P., 2005. Thermo-FTIR Spectroscopy Analysis as a Method of Characterizing Ancient Ceramic Technology. J. Therm. Anal. Calorim. 82, 609–616.
Shoval, S., Erez, Z., Kirsh, Y., Deutsch, Y., Kochavi, M., Yadin, E., 1989. Determination of the Intensity of an Early Iron Age Conflagration at Tel-Hadar, Israel. Thermochimica Acta 148, 485–492.
Shoval, S., Paz, Y., Analyzing the fired-clay ceramic of EBA Canaanite pottery using FT-IR spectroscopy and LA-ICP-MS. Period. Mineral. 84: 213–231.
Smith, P., 2004. Skeletal Remains from Level VI, in: Ussishkin, D. (Ed.), The Renewed Archaeological Excavations at Lachish (1973–1994). Institute of Archaeology, Tel Aviv University, Tel Aviv, pp. 2504–2507.
Stevanović, M., 1997. The Age of Clay: The Social Dynamics of House Destruction. J. Anthropol. Archaeol. 16, 334–395.
Stiros, S.C., 1996. Identification of Earthquakes from Archaeological Data: Methodology, Criteria and Limitations. In: Stiros, S.C., Jones, R.E. (Eds.), Archaeoseismology. British School at Athens, Athens, pp. 129–152.
Stordeur, D., Brenet, M., der Aprahamian, G., Roux, J.C., 2000. Les bâtiments communautaires de Jerf el Ahmar et Mureybet Horizon PPNA (Syrie). Paléorient 26, 29–44.
Tipper, J., 2012. Discussion. In: Tipper, J. (Ed.), Experimental Archaeology and Fire: The Investigation of a Burnt Reconstruction at West Stow Anglo-Saxon Village. Suffolk County Council Archaeological Service, Bury St Edmunds, pp. 142–173.
Toffolo, M.B., Boaretto, E., 2014. Nucleation of Aragonite upon Carbonation of Calcium Oxide and Calcium Hydroxide at Ambient Temperatures and Pressures: A New Indicator of Fire-Related Human Activities. J. Archaeol. Sci. 49, 237–248.
Tufnell, O., 1958. Lachish IV (Tell ed-Duweir): The Bronze Age. Oxford University Press, London.
Twiss, K.C., Bogaard, A., Bogdan, D., Carter, T., Charles, M.P., Farid, S., Russell, N., Stevanović, M., Yalman, E.N., Yeomans, L., 2008. Arson or Accident? The Burning of a Neolithic House at Çatalhöyük, Turkey. J. Field Archaeol. 33, 41–57.
Ussishkin, D., 2004a. A Synopsis of the Stratigraphical, Chronological and Historical Issues, in: Ussishkin, D. (Ed.), The Renewed Archaeological Excavations at Lachish (1973–1994). Institute of Archaeology, Tel Aviv University, Tel Aviv, pp. 50–119.
Ussishkin, D., 2004b. Area P: The Level VI Temple, in: Ussishkin, D. (Ed.), The Renewed Archaeological Excavations at Lachish (1973–1994). Institute of Archaeology, Tel Aviv University, Tel Aviv, pp. 215–281.
Ussishkin, D., 2004c. Area GE: The Inner City-gate, in: Ussishkin, D. (Ed.), The Renewed Archaeological Excavations at Lachish (1973–1994). Institute of Archaeology, Tel Aviv University, Tel Aviv, pp. 624–689.
Verhoeven, M., 2000. Death, Fire and Abandonment: Ritual Practice at Late Neolithic Tell Sabi Abyad, Syria. Archaeol. Dialogues 7, 46–65.
Villagran, X.S., Strauss, A., Miller, C., Ligouis, B., Oliveira, R., 2017. Buried in Ashes: Site Formation Processes at Lapa do Santo Rockshelter, East-central Brazil. J. Archaeol. Sci. 77, 10–34.
Waiman-Barak, P., Susnow, M., Nickelsberg, R., Cline, E.H., Yasur-Landau, A., Shahack-Gross, R., 2018. Technological Aspects of Middle Bronze Age II Production of Pithoi at Tel Kabri, Israel: Specialized Pottery Production in a Palatial System. Levant 50, 32–51.

Walton, W.D., Thomas, P.H., 2002. Estimating Temperatures in Compartment Fires. In: DiNenno, P.J., Drysdale, D., Beyler, C.L., Walton, W.D., Custer, R.L.P., Hall, J.R.J., Watts, J.M.J. (Eds.), SFPE Handbook of Fire Protection Engineering. National Fire Protection Association, Quincy, MA, pp. 3.171–3.188.
Weiner, S., 2010. Microarchaeology: Beyond the Visible Archaeological Record. Cambridge University Press, Cambridge.
Weissbein, I., Garfinkel, Y., Hasel, M.G., Klingbeil, M.G., Brandl, B., Misgav, H., 2019. The Level VI North-East Temple at Tel Lachish. Levant 51, 76–104.
Wright, G.R.H. 1985. Ancient building in South Syria and Palestine. Brill, Leiden.
Wileman, J, 2009. War and Rumors of War: The Evidential Base for Recognition of Warfare in Prehistory. Archaeopress, Oxford.
Yoshioka, S., Kitano, Y., 1985. Transformation of Aragonite to Calcite through Heating. Geochimical J. 19, 245–249.
Zuckerman, S., 2007. Anatomy of a Destruction: Crisis Architecture, Termination Rituals and the Fall of Canaanite Hazor. J. Mediterr. Archaeol. 20, 3–32.